

T. Mergner · G. Schweigart · C. Maurer · A. Blümle

Human postural responses to motion of real and virtual visual environments under different support base conditions

Received: 30 September 2004 / Accepted: 10 May 2005 / Published online: 18 August 2005
© Springer-Verlag 2005

Abstract The role of visual orientation cues for human control of upright stance is still not well understood. We, therefore, investigated stance control during motion of a visual scene as stimulus, varying the stimulus parameters and the contribution from other senses (vestibular and leg proprioceptive cues present or absent). Eight normal subjects and three patients with chronic bilateral loss of vestibular function participated. They stood on a motion platform inside a cabin with an optokinetic pattern on its interior walls. The cabin was sinusoidally rotated in anterior–posterior (a–p) direction with the horizontal rotation axis through the ankle joints ($f=0.05\text{--}0.4\text{ Hz}$; $A_{\max}=0.25^{\circ}\text{--}4^{\circ}$; $v_{\max}=0.08\text{--}10^{\circ}/\text{s}$). The subjects' centre of mass (COM) angular position was calculated from optoelectronically measured body sway parameters. The platform was either kept stationary or moved by coupling its position 1:1 to a–p hip position ('body sway referenced', BSR, platform condition), by which proprioceptive feedback of ankle joint angle became inactivated. The visual stimulus evoked inphase COM excursions (visual responses) in all subjects. (1) In normal subjects on a stationary platform, the visual responses showed saturation with both increasing velocity and displacement of the visual stimulus. The saturation showed up abruptly when visually evoked COM velocity and displacement reached approximately $0.1^{\circ}/\text{s}$ and 0.1° , respectively. (2) In normal subjects on a BSR platform (proprioceptive feedback disabled), the visual responses

showed similar saturation characteristics, but at clearly higher COM velocity and displacement values ($\approx 1^{\circ}/\text{s}$ and 1° , respectively). (3) In patients on a stationary platform (no vestibular cues), the visual responses were basically similar to those of the normal subjects, apart from somewhat higher gain values and less-pronounced saturation effects. (4) In patients on a BSR platform (no vestibular and proprioceptive cues, presumably only somatosensory graviceptive and visual cues), the visual responses showed an abnormal *increase* in gain with increasing stimulus frequency in addition to a displacement saturation. On the normal subjects we performed additional experiments in which we varied the gain of the visual response by using a 'virtual reality' visual stimulus or by applying small lateral platform tilts. This did not affect the saturation characteristics of the visual response to a considerable degree. We compared the present results to previous psychophysical findings on motion perception, noting similarities of the saturation characteristics in (1) with leg proprioceptive detection thresholds of approximately $0.1^{\circ}/\text{s}$ and 0.1° and those in (2) with vestibular detection thresholds of $1^{\circ}/\text{s}$ and 1° , respectively. From the psychophysical data one might hypothesise that a proprioceptive postural mechanism limits the visually evoked body excursions if these excursions exceed $0.1^{\circ}/\text{s}$ and 0.1° in condition (1) and that a vestibular mechanism is doing so at $1^{\circ}/\text{s}$ and 1° in (2). To better understand this, we performed computer simulations using a posture control model with multiple sensory feedbacks. We had recently designed the model to describe postural responses to body pull and platform tilt stimuli. Here, we added a visual input and adjusted its gain to fit the simulated data to the experimental data. The saturation characteristics of the visual responses of the normals were well mimicked by the simulations. They were caused by central thresholds of proprioceptive, vestibular and somatosensory signals in the model, which, however, differed from the psychophysical thresholds. Yet, we demonstrate in a theoretical approach that for condition (1) the model can be made monomodal proprioceptive with the psychophysical

T. Mergner (✉) · G. Schweigart · C. Maurer
Neurological University Clinic, Neurocenter,
Breisacher Str. 64, 79106 Freiburg, Germany
E-mail: mergner@uni-freiburg.de
Tel.: +49-761-2705313
Fax: +49-761-2705310

A. Blümle
German Cochrane Center,
Institute of Biometry and Med. Informatics,
Stefan-Meier-Strasse 26, 79104 Freiburg, Germany
E-mail: bluemle@cochrane.de
Tel.: +49-761-2036715
Fax: +49-761-2036712

0.1°/s and 0.1° thresholds, and for (2) monomodal vestibular with the psychophysical 1°/s and 1° thresholds, and still shows the corresponding saturation characteristics (whereas our original model covers both conditions without adjustments). The model simulations also predicted the almost normal visual responses of patients on a stationary platform and their clearly abnormal responses on a BSR platform.

Keywords Multi-sensory interaction · Visual stimulation · Saturation · Vestibular loss · Postural control · Detection threshold · Human

Introduction

Human upright stance is controlled with the help of several senses. Important information is provided by vision, which normally combines with cues from other senses, i.e. mainly from the vestibular, proprioceptive and somatosensory systems. Motion of the visual scene has long been known to induce postural reactions in human subjects (Lee and Lishman 1975; Lestienne et al. 1977; Dichgans and Brandt 1979; Paulus et al. 1984). A wide variety of moving visual stimuli have been employed to study this phenomenon such as tilting or swinging rooms (Lee and Lishman 1975; Bles et al. 1983) or projected displays simulating a moving visual scene (Lestienne et al. 1977; van Asten et al. 1988), to name a few. Furthermore, various procedures were employed to enhance the effect of the visual stimulus, for instance, by having subjects stand on an unstable base of support (see below). Actually, in most situations of everyday life the visual scene is not moving, but is stationary, and it then serves as a space reference. Yet, the studies in which motion of a visual scene was used as a stimulus yielded a number of interesting findings which may help us better to understand how humans control their upright stance. We also used this approach in the present study and, therefore, briefly describe the most relevant findings from the literature.

Previous researchers noted a pronounced saturation of the visually evoked body excursion (visual response) when increasing the stimulus amplitude (Bles et al. 1980, 1983; Lestienne et al. 1977; van Asten et al. 1988; Peterka and Benolken 1995). During sinusoidal stimulation, the higher the stimulus frequency, the earlier the occurrence of saturation (range, 0.1–0.5 Hz; Peterka and Benolken 1995). Furthermore, already below the range of pronounced saturation, the response was proportional to the logarithm of stimulus amplitude (Lestienne et al. 1977; Peterka and Benolken 1995). The response characteristics are generally related to three factors. One factor is the dynamics of the body's biomechanics, which show a low-pass filter behaviour (see Nashner 1972). But this factor does not explain the saturation effects. The second factor is the low-pass characteristics of the sensory channel for visual motion and its tendency for

saturation, as one may infer them from the optokinetic eye reflex with its low-pass behaviour and velocity saturation (see Barnes 1993; Schweigart et al. 1999, 2003). The third, and probably the most relevant, factor is an interaction between the visual signal and the other sensory cues. When the moving visual stimulus induces a body excursion, non-visual cues (vestibular, proprioceptive and somatosensory) are activated and tend to counteract the excursion in an attempt to maintain primary body position, i.e. body uprightness.

The presumed intersensory interaction was addressed in a number of previous studies which modified the visual response by manipulating the non-visual cues. Some investigators weakened the effect of plantar somatosensory cues on the visual response by having subjects stand on a compliant support base in the form of foam rubber and, thereby, enhanced the visual response (e.g. Amblard et al. 1985; Norre 1993; Lord and Menz 2000). Other studies showed that somatosensory loss of the feet due to polyneuropathy tends to enhance the visual response (e.g. Kotaka et al. 1986). Furthermore, an increase of the visual response was observed after functionally immobilising the ankle joints and, thereby, largely reducing the feedback from ankle joint proprioceptors (Peterka and Benolken 1995; Peterka 2002; this was achieved by coupling the tilt angle of the support base 1:1 to the body tilt angle, a manipulation which is often referred to as a 'body sway referencing' of the support base). Finally, loss of vestibular function has also been shown to enhance the visual response (e.g. Bles et al. 1983; Peterka and Benolken 1995; Peterka 2002). Thus, there is clear evidence for the presumed interaction.

However, the interaction per se does not explain the saturation behaviour of the visual response. Given that the signal processing in the postural control system was linear, the presumed interactions would yield a lowered gain of the visual response, but the gain would be constant. A response with decreasing gain (saturation) upon increasing stimulus amplitude indicates a non-linearity in the signal processing. This can directly be due to a saturation mechanism (limitation of signal magnitude) or indirectly result from a detection threshold somewhere in the network or from interactions between signals which do not follow the superposition law (such as a multiplication, for instance). One can draw from the literature evidence for each of these non-linear mechanisms. For instance, as mentioned before, the visual signal for the optokinetic eye response is thought to show a saturation (see Barnes 1993; Schweigart et al. 1999) and vestibular-visual interaction for self-motion perception is thought to contain thresholds and a non-linear suppression mechanism (Mergner et al. 2000a). Furthermore, non-visual postural responses, i.e. responses to vestibular and somatosensory stimuli, show a decreasing gain with increasing stimulus magnitude (Peterka 2002; Mergner et al. 2003). This behaviour has been mimicked in previous studies which used simulations of dynamic postural control models that contained

either central threshold elements (Mergner et al. 2003) or non-linear inter-sensory interaction mechanisms (van der Kooij et al. 2001).

We studied the saturation of the visual response for three reasons. The first reason is that the study of the non-linear properties of a sensorimotor system may generally help to understand the system better. It is true that the non-linearities are a nuisance when one tries to describe the systems' behaviour by means of explicit mathematical formulas, but they do not represent a hurdle for model simulation of the system. They may even be helpful in the modelling process when it comes to disambiguating the presumed internal structure of the neural mechanism under investigation.¹

The second reason for studying the saturation is that the previous work suggested that it may be related to detection thresholds known for self-motion perception (Peterka and Benolken 1995). If tested in an experimental situation where body stabilisation appears to depend mainly on vestibular cues, the saturation occurs when the visually evoked body excursion reaches a velocity of approximately 1°/s, a value which corresponds to the vestibular detection thresholds reported in psychophysical studies (Benson et al. 1989; Mergner et al. 1991; Fitzpatrick and McCloskey 1994). How to explain this congruency between action (posture control) and perception? Is it possible that detection thresholds of this relatively high magnitude are involved in posture control?

The third reason is that central threshold mechanisms have been implemented in a recent sensory feedback model of posture control (Mergner et al. 2003). With the help of the thresholds, we were able to describe in model simulations the non-linear responses we observed with body pull and platform tilt stimuli. We, therefore, asked here whether these thresholds can also explain the saturation of the visual response. Interestingly, however, the thresholds in the model are considerably smaller than the psychophysical thresholds described earlier. This could suggest that the psychophysical thresholds do not lend themselves to a simple and straightforward explanation of the postural data.

These considerations led us to investigate the postural responses evoked by visual stimulation under various experimental conditions and compare the saturation characteristics of these responses to the known psychophysical threshold data and to simulations of our postural control model.

To this end, we studied the postural responses during sinusoidal rotations of a 'real world' visual scene (subjects were inside a pivotable cabin with optokinetic patterns on its interior walls). The rotations were per-

formed in the anterior–posterior (a–p) plane with different stimulus frequencies and amplitudes. The stimuli were applied under various experimental conditions. In a series of experiments we varied the other sensory cues, i.e. the visual response was evoked in the presence versus the absence of vestibular cues and of ankle joint proprioceptive cues. The role of the vestibular cues was investigated by comparing the responses of normal subjects with those of patients with loss of vestibular function. The effect of the proprioceptive cues was investigated by testing the subjects on a stationary platform versus a 'body sway referenced' (BSR) platform (see above). In other experiments, we aimed selectively to modify the strength of the visual effect without altering the other sensory cues. We did so in two ways. In one subset of experiments we replaced the 'real world' visual stimulus by a 'virtual reality' one, after pilot experiments had suggested that the latter is less effective in evoking postural responses. In the other subset we superimposed on the a–p visual stimuli small tilts of the platform, which were oriented laterally (thus perpendicular to the visual stimulus). Pilot experiments had indicated that this procedure leads to a gain enhancement of the visual response that cannot be explained by a mechanical cross-talk.

In the data analysis, we assessed visual response gain as a function not only of stimulus frequency, but also of stimulus velocity and displacement, having in mind that the saturation of the visual responses may be determined by the velocity and/or displacement thresholds in the postural control loop (see above). For the comparison between model simulations and experimental data, we had to extend our postural control model by a visual system, which so far was not implemented. However, we kept this addition simple, abandoning at present the implementation of visual interactions with other cues at sensory levels. Instead, we adjusted visual gain in the simulations in an attempt to fit the simulated to the experimental data. Details of the model and the simulations are given in Appendix.

Methods

Subjects

Eight normal subjects and three patients with bilateral loss of vestibular functions participated. The age of normals was 34.4 ± 9.9 years (mean \pm 1SD; 3 women, 32.3 ± 2.5 years; 5 men, 35.6 ± 12.7 years) and that of patients 36.0 ± 1.4 years (all men). Vestibular dysfunction in the patients was assessed by clinical examination (e.g. balancing problems when standing on foam rubber with eyes closed), electronystagmography (absence of caloric nystagmus and of rotation-evoked vestibulo-ocular reflex) and case histories (meningitis and ototoxic medication in childhood). Apart from vestibular loss and hearing impairment, patients showed no other health problems. The study was ap-

¹When making inferences from the input–output behavior of a neural system on its internal structure in order to model this, the arrangement of the internal processing elements is arbitrary as long as they behave linearly. Non-linear elements may help to disambiguate the problem, because their arrangement within the network influences the output. This may be highly relevant when there are limitations to the experimental dissection of a system.

proved by the local ethics committee and performed in accordance with the ethical standards of the Declaration of Helsinki (revised Edinburgh 2000). All subjects gave their informed consent prior to their inclusion into the study.

Set-up, platform conditions

Subjects stood upright on a custom-built motion platform and were presented with a visual motion stimulus in the sagittal plane (see next section). Subjects stood with their feet shoulder-width apart from each other. They held their hands up to the shoulder level, with each hand holding a grip fixed to a rope that was loosely hanging from the ceiling. Moving the hands down put tension on the ropes and thereby allowed subjects to stabilise themselves in case they felt their body equilibrium severely endangered (this occasionally happened with the vestibular loss patients; the trials were finished and taken as ‘falls’). In the hands-up position, subjects did not obtain considerable somatosensory spatial orientation cues from this safety set-up.

The motion platform rested on six ‘legs’, each incorporating a motor capable of producing a change in the length of the leg (hexapod with Stuart principle). The motors were controlled by a computer which allowed to generate platform motion in 6-D (3-D rotations, 3-D translations). In some experiments of the present study, the stimulus condition included platform tilt in the sagittal plane (a–p direction, pitch) or frontal plane (lateral direction, roll) with the axes at the level of the subjects’ foot soles. Three different conditions of the motion platform were used:

1. *Platform stationary*. The platform was kept horizontal and stationary.
2. *Platform ‘body sway referenced’, BSR*. The platform angular position was coupled 1:1 to subjects’ hip angular position in the a–p plane (hip angle measured optoelectronically, see below; delay time, <60 ms). The condition started from a primary position in which the motion platform was level and subjects’ bodies were approximately upright. By means of this procedure, the angle of the ankle joint was continuously kept at $\approx 90^\circ$. This essentially abolishes ankle joint proprioceptive feedback (change of body-to-foot angle, i.e. ankle joint angle, always was <5% of that of body-in-space angle). Noticeably, postural stabilisation in this condition is to be performed by solely adjusting the ankle torque and not the ankle angle while on a stationary support surface both adjustments tend to be coupled.
3. *Platform tilted laterally*. In order to mimic an “unstable” body support (and by this to enhance the visual effect; see [Introduction](#)), the platform was tilted in the roll plane, i.e. perpendicular to the visual motion stimulus, with continuous sinusoidal tilts of $\pm 0.2^\circ$ at 0.25 Hz. In this condition, normal subjects

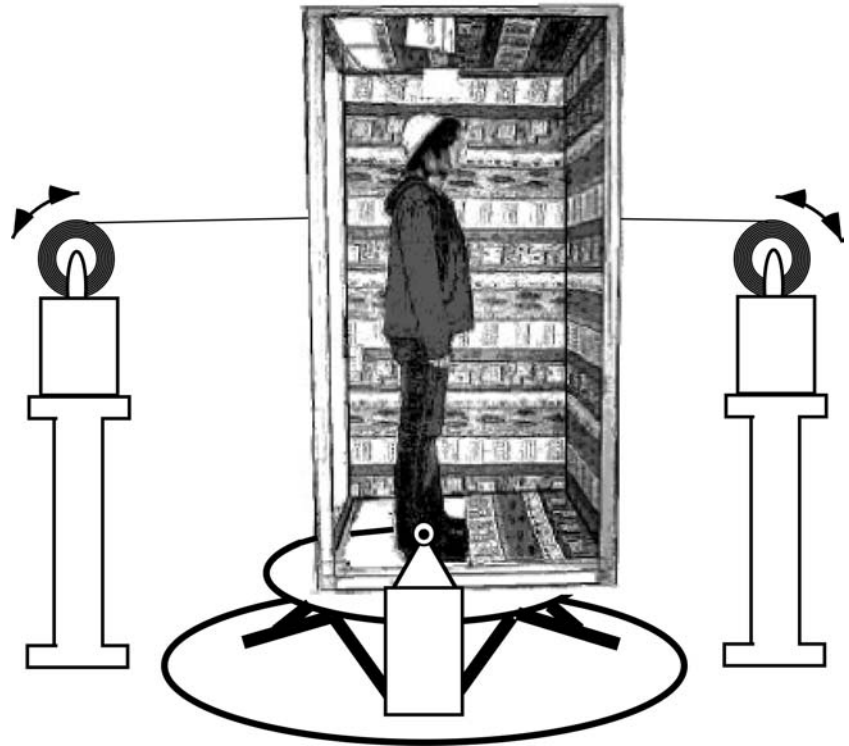
reported on request that they sensed the very small platform tilts most of the time but intermittently became unaware of it. The tilts led them to experience the body support surface as “slightly unstable”.

Visual stimulation

Two different visual stimuli were used in separate experiments:

1. *‘Real world’ visual stimulus*. While standing on the platform, subjects viewed the inside of a cabin with a full-field optokinetic pattern (‘real world’ visual scene, “full field”; Fig. 1). The cabin measured 100 cm \times 80 cm \times 190 cm (depth \times width \times height) and consisted of a thin aluminium frame with styro-foam walls. The interior of the walls were covered by a wallpaper printed with horizontal stripes of different colours, brightness, contrast and height (2–15 cm), which were interspersed with patches and other horizontal and vertical ornamental patterns. During stimulation, the outside laboratory was darkened and the visual scene on the inside was illuminated by two electric bulbs attached to the cabin ceiling. In the primary position, the subjects’ eye-to-pattern distance was 60 cm. The light-weight cabin could be rotated about an axis through the subjects’ ankle joints (thus producing the same relative motion between the subjects and scene as during subjects’ own spontaneous a–p body sway about the ankle joints). The movements were generated, under computer control, independently of the motion platform, with the help of two servo-controlled cable winches with no perceivable noise or vibration and with an accuracy error of <3% of stimulus amplitude. Subjects were given the instructions to keep their gaze near the centre of the scene and always to remain upright.
2. *‘Virtual reality’ stimulus*. In parts of the experiments, subjects viewed instead of the ‘real world’ scene a 3-D ‘virtual reality’ scene (Mergner et al. 1997). It was back-projected onto a semi-transparent screen with the help of a video projection system (Barcographics 808; Barco N.V., Kortrijk, Belgium). The scene was generated in an Onyx Reality Engine II computer (Silicon Graphics, Mountain View, CA, USA) using the software Relax, version 2 (MediaSystems, Karlsruhe, Germany). The scene consisted of the interior of a room with a shelf, furniture and a variety of ornamental patterns. It was viewed by the subjects through shutter glasses for 3-D vision (CrystalEYES Model CE-PC; StereoGraphics, San Rafael, CA, USA; alternating frequency, 120 Hz). In subjects’ primary body position, the distance from the eyes to the projection screen was 80 cm. The subjects’ visual field was restricted by the shutter glasses to $90^\circ \times 66^\circ$ ($w \times h$). The scene was tilted in the sagittal plane about the same axis as the ‘real world’ stimulus.

Fig. 1 Experimental set-up showing the 'real world' visual scene in a cabin which was moved by two cable winches about an axis through the subjects' ankle joints (one side wall of the cabin was removed in order to take the picture). Subjects stood on a motion platform which could be tilted by a hexapod system



The 'virtual reality' stimulus was presented in two different versions: (a) '*Mental task*' version. The scene contained in the centre region a virtual yellow disc (diameter, 6°) which followed a pseudo-random trajectory in the frontal plane at a virtual distance of 2.4 m. 2-D movements of it were generated by superimposing two sine wave stimuli (frequencies, 0.24 and 0.85 Hz) in up-down and medio-lateral directions with varying phase values. These movements of the disc were independent of the a-p tilt movements of the virtual room. The disc allowed us to present subjects with a simple mental task, in addition to the task of always standing upright. They were to read aloud black numbers from zero to nine which appeared on the disc in random order at time intervals of 2.5–3.0 s in one of eight possible frontal orientations (e.g., upside down). By this task we tried to bind the subjects' attention and to control their gaze direction so that they no longer directly viewed and attended the moving scene. (b) '*No mental task*' version. The scene was presented without the moving disc and numbers. Subjects were instructed to look into the virtual room and to keep their gaze near the centre of the scene, while keeping the body upright.

Both the real and the virtual visual scenes were sinusoidally tilted in the a-p plane at four different frequencies ($f = 0.05, 0.1, 0.2, 0.4$ Hz) and with five different peak angular excursions ($A_{\max} = \pm 0.25^\circ, \pm 0.5^\circ, \pm 1^\circ, \pm 2^\circ$ and $\pm 4^\circ$; total of 20 different stimuli), which yielded peak velocities in the range of $v_{\max} = 0.08$ to $10^\circ/s$. The stimuli were presented in trials that lasted 80 s, with the number of sine wave cycles in each trial depending on stimulus frequency.

Procedures and recordings

With each experiment, four experimental sessions were performed, each testing one of the four frequencies. Each session contained three different runs, one for each of the three platform conditions. Each run contained one trial for the five different stimulus amplitudes. Sessions, runs and trials were presented in random order. In each trial, onset and offset of the sinusoidal visual stimuli were smoothed by starting from and ending at the primary position with a cosine trajectory and by presenting during the first and last half cycle, respectively, only half of the desired amplitude/velocity (see Fig. 2a–c; primary position: visual vertical of room, corresponding to space vertical). Subjects were given short breaks between trials (ca. 15 s) and longer breaks between runs (1–3 min, with the possibility of sitting). During the trials the subjects' ears were plugged to minimise auditory cues.

Recordings comprised the positions of the subjects' hips and shoulders and of the platform and the 'real world' visual scene with the help of an optoelectronic device (Optotrak 3020, Waterloo, Canada; spatial resolution, 0.2 mm). To this end, we used rigid plastic triangles on which three active markers of the recording system were fixed. The triangles were attached to the subjects' hips and shoulders, to a rigid bar on the platform and to the cabin used for the 'real world' stimulus. A PC calculated online 3-D translational and 3-D angular positions of the triangles. The data were stored on a hard disc for offline analysis (see below). The computer, by which the 'virtual reality' visual stimulus

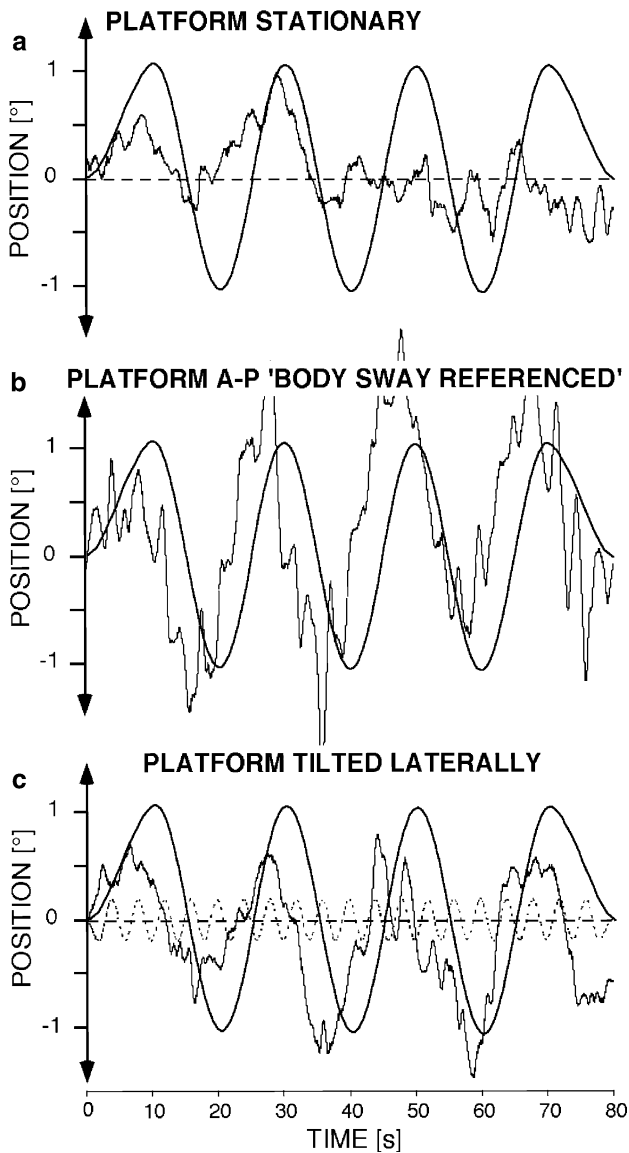


Fig. 2 Examples of a normal subject's postural responses evoked by the 'real world' visual stimulus for the three platform conditions indicated (a–c). Time series of angular position of the visual stimulus (sine-like curves with smoothed onset and offset, 0.05 Hz, $\pm 1^\circ$), of subjects' centre of mass (COM, *thin full lines*) and of platform (*dashed*) in anterior–posterior plane (a–p). Platform was either stationary (a), coupled 1:1 to body position (b; 'body sway referenced', BSR platform; trace equals COM trace) or sinusoidally tilted in lateral direction (frontal plane; c; 0.25 Hz, $\pm 0.2^\circ$; *small dotted sine wave*)

was created, delivered in addition an analogue signal that reflected the angular position of the stimulus in analogy to the 'real world' stimulus.

Data analysis

Hip, shoulder, platform and visual stimulus position signals were transferred online to a computer system via an analog–digital converter at a sampling rate of 100 Hz. The data were recorded with a software pro-

grammed in LabView (National Instruments, Austin, TX, USA). Analyses were performed offline with custom-made software programmed in MATLAB (The MathWorks Inc., Natick, MA, USA; this program was also used for model simulations and optimising procedures, see Appendix). From the data of the shoulder-to-hip and hip-in-space angular displacements we calculated the a–p angular displacement in space of the centre of mass (COM) of subjects' bodies according to the anthropometric data of Winter (1990). Because the shoulder-to-hip angular displacements turned out to be extremely small, the calculated COM excursions closely resembled the measured hip excursions. We, therefore, used the hip excursion to represent the COM excursions and neglected the small movements in the hip joint. Also the translatory vertical hip movements were very small by which we could exclude that subjects performed considerable knee bending.

The subjects' responses in the sagittal plane to the sinusoidal visual stimuli were quantified by calculating the amplitude (peak angular displacement) and phase values of the fundamental waves of the stimuli and the responses (COM excursions) using Fast Fourier Transformation (FFT; we ascertained that the power of the response fundamental was larger than the first/second harmonic by a factor of 3/6 across all stimulus amplitudes and frequencies used). Phase was taken from the temporal relationship between response and stimulus fundamentals (in degrees; 0° , no phase shift; positive values, lead; negative values, lag). Gain values were taken from the ratio of the amplitudes of the response and the stimulus fundamentals. For example, with a COM excursion in perfect alignment with the visual scene, gain would amount to unity and phase to 0° . The first and the last cycle of each trial were not evaluated. With the 80 s trial duration 2 cycles were evaluated for the 0.05 Hz trial, 6 for 0.1 Hz, 14 for 0.2 Hz and 30 for 0.4 Hz. The data from these cycles in a trial were averaged (yielding one response gain and phase value per subject and stimulus condition). From these values we present in the following 'grand averages' across subjects with the error bars representing the inter-individual variability (1 SD). Statistics was performed using the statistics program StatView (SAS Inc., Cary, NC, USA). Statistical significance was tested by analysis of variance (ANOVA).

Results

'Real world' visual stimulus

Normal subjects

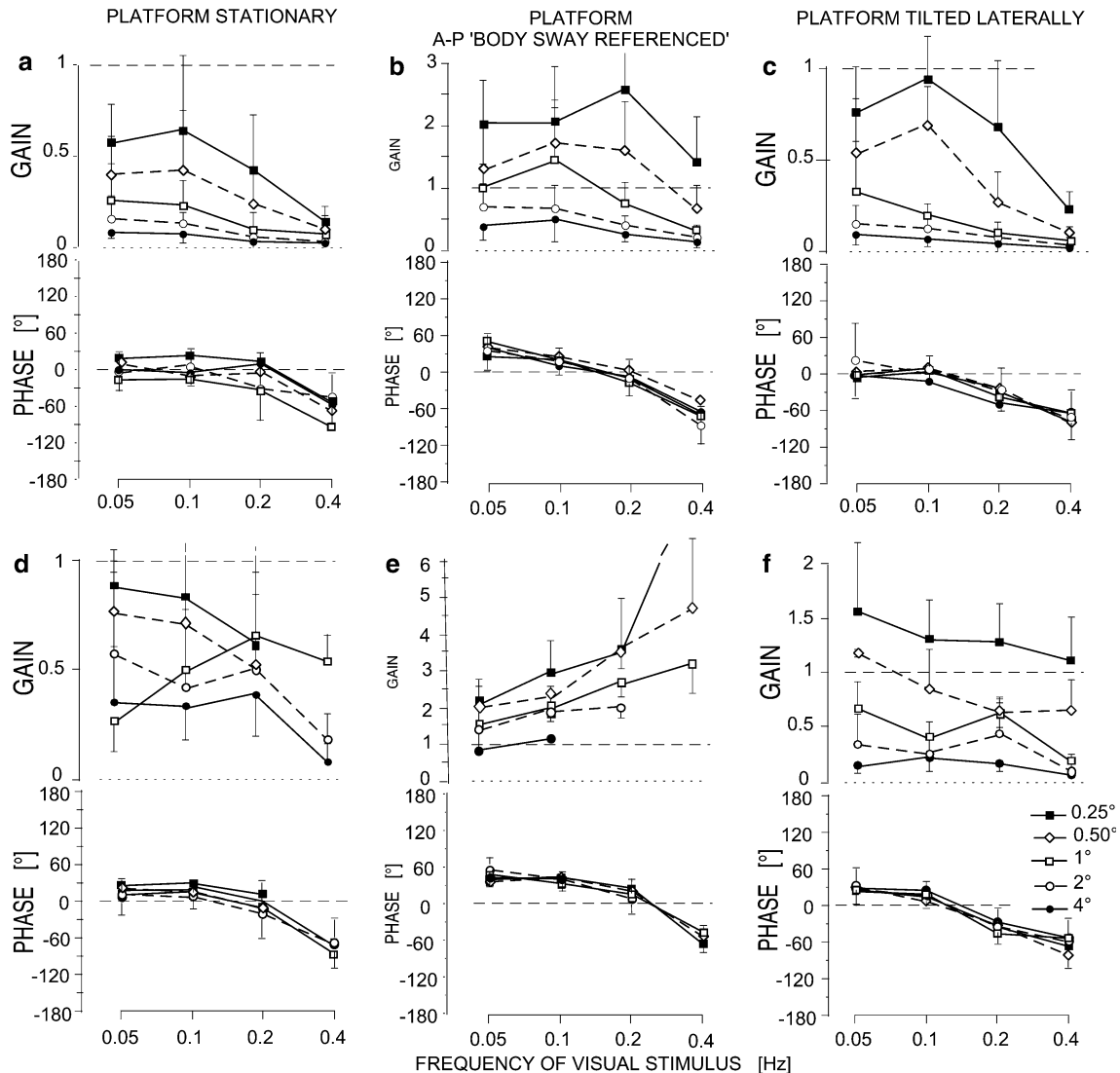
Figure 2a–c shows typical examples of a normal subject's visual response, i.e. the COM a–p angular excursion during sinusoidal a–p rotations of the 'real world' visual scene (0.05 Hz, $\pm 1^\circ$) for the three different platform conditions used. In panel a, the *platform* was *sta-*

tionary. Note that the visual response is relatively small as compared to the subject's spontaneous sway (therefore averaged data was used for analysis; see [Methods](#)). The example in panel b is taken from the experiments with 'body sway referenced' (BSR) platform. The visual response is clearly larger than before and approximately as large as the stimulus (and is slightly leading it). In panel c, small lateral platform tilts were superimposed on the a-p visual stimulus ('laterally tilted' platform; $\pm 0.2^\circ$, 0.25 Hz, i.e. a frequency not tested with the visual stimulus). The visual response is slightly larger than in the stationary platform condition.

In the following, we present the visual responses in terms of mean gain and phase (grand averages across subjects) as a function of stimulus frequency, velocity and amplitude. It is true that these three stimulus parameters are related to each other during sinusoidal stimulation (velocity co-varies with both frequency and amplitude). Yet, our aim was to discern the effects of frequency (i.e. gain changes associated with corresponding phase changes due to filter properties) from the effects due to amplitude and/or velocity saturation (gain changes without phase changes). We compare these effects across the three platform conditions where ankle joint proprioception was either present (stationary platform) or absent (BSR platform) or where a superposition of lateral platform tilt increased the gain of the visual response (see [Introduction](#)).

Gain and phase over stimulus frequency In Fig. 3a (upper panel) gain of the visual response is plotted over the four stimulus frequencies for the stationary platform condition. The lower panel gives the corresponding phase values. The five response curves in each panel give

Fig. 3 Gain and phase of postural response (visually evoked COM excursion) plotted over stimulus frequency, separately for the five different amplitudes of the visual stimulus ('real world'). Mean values (and 1SD) of normal subjects (a-c) and vestibular loss patients (d-f) are given for the three different platform conditions as indicated. Note different scales on ordinates. For clarity, phase SD bars are given only for the $\pm 2^\circ$ stimulus



the data for the five different stimulus amplitudes, as indicated. Both gain and phase varied with stimulus frequency. Gain decreased with increasing frequency and phase developed a lag (starting from a slight lead at 0.05 Hz and reaching -61° at 0.4 Hz, compatible with low-pass filter characteristics). This similarly applied to the five gain and phase curves. However, gain, unlike phase, also depended on stimulus amplitude. The gain curve for the largest stimulus amplitude (4°) showed the lowest values (0.03–0.08) and that for the smallest amplitude ($\pm 0.25^\circ$) the highest values (range: 0.14–0.65).

Qualitatively similar data were obtained in the other two platform conditions. In the 'BSR' platform condition (Fig. 3b) gain was overall increased by a factor of 2–5. It tended to decrease at high stimulus frequency with the phase showing a lag (averages across all stimulus amplitudes: 0.05 Hz: 39° ; 0.1 Hz: 19° ; 0.2 Hz: -18° ; 0.4 Hz: -69°). The gain curves for the different stimulus amplitudes showed a decrement with increasing amplitude, while the corresponding phase curves remained essentially the same, which is similar to the phase behaviour on the stationary platform.

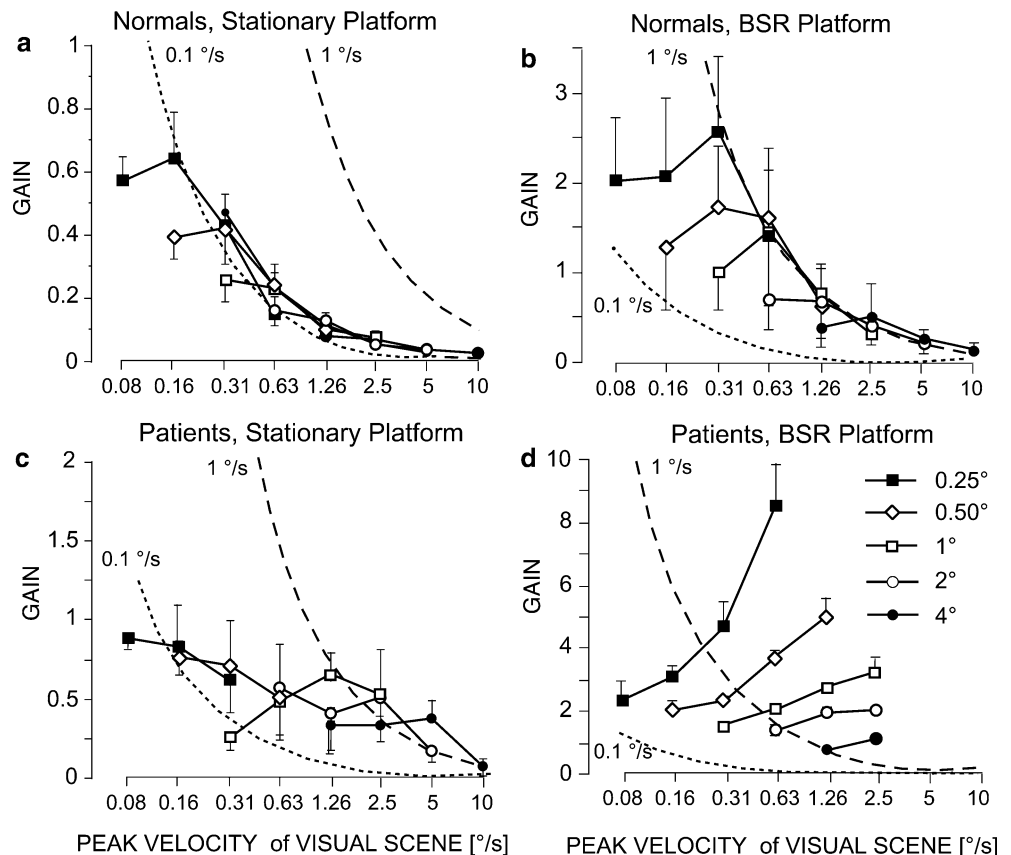
With a *laterally tilted platform* (Fig. 3c) gain was slightly larger than with a stationary platform. The gain increase applied to a considerable extent only to the $\pm 0.25^\circ$ and $\pm 0.5^\circ$ stimuli, where it reached 43% on an average. (A possible explanation is that with the larger visual stimuli the subjects tended to perceive the lateral

tilt no longer.) The phase curves were essentially similar to those obtained on the stationary platform. The gain increase was not directly related to the mechanical aspects of the lateral tilt. Gain of the a–p COM excursions in relation to the lateral platform tilt was close to zero (FFT response fundamental in relation to stimulus fundamental at 0.25 Hz; not shown). Vice versa, the a–p visual stimulus also affected the COM response to the lateral platform tilt only in an indirect (non-mechanical) way, a finding which will be published separately.

Taken together, the visual responses in the three platform conditions showed a clear dependency on stimulus frequency with a gain decrease and phase lag at 0.4 Hz. This frequency dependency is similar to that previously observed with the tilt and pull stimuli in the absence of vision (Peterka 2002; Mergner et al. 2003). Therefore, it appears to reflect mainly the low-pass filter dynamics of the postural system, here possibly in combination with low-pass characteristics of the visual signal. The responses showed, in addition, a clear saturation behaviour in relation to stimulus amplitude. In the following, we try to discern to what extent this effect is due to a velocity and/or a displacement non-linearity.

Gain over stimulus velocity Gain over peak stimulus velocity is shown in Fig. 4a for the *stationary platform* condition. As before, we show five gain curves for each of the five different stimulus amplitudes with the frequency being increased in each curve (the phase curves

Fig. 4 Gain plots over peak stimulus velocity of the visual responses in normal subjects (**a, b**) and in patients (**c, d**) ('real world' stimulus). Mean values (and 1SD) are given separately for the five different stimulus amplitudes. **a, c** Stationary platform. **b, d** 'Body sway referenced', BSR platform. Note different ordinate scales. Dashed and dotted curves in each panel show for comparison theoretical curves of COM excursions with peak velocity of 1°/s and 0.1°/s, respectively



are no longer considered since they did not vary to a considerable extent with stimulus magnitude). Note that gain decreases within each curve as well as across curves with increasing stimulus velocity, yielding the picture of an essentially hyperbolic decay. When we calculated a gain curve that would result if the COM excursion always had $0.1^\circ/\text{s}$ peak velocity irrespective of stimulus amplitude and added it to the graph (dotted curve in Fig. 4a), the decay of this calculated curve coincided rather well with that of the experimental data. The findings, therefore, suggest that the visually evoked COM excursions tend to saturate when they reach a velocity of approximately $0.1^\circ/\text{s}$.

Qualitatively similar findings were obtained for the other two platform conditions. With the *BSR platform* (Fig. 4b), gain was considerably higher overall. Yet, the gain curves showed similar saturation characteristics as before, in that the gain curves start to decay along a common limit trajectory once peak velocity has reached the critical value defined by this limit. However, the velocity limit is now larger by a factor of 10 as compared to the stationary platform condition, i.e. it amounts to about $1^\circ/\text{s}$ (dashed curve in Fig. 4b). Thus, Fig. 4b indicates that COM velocity in the 'BSR' platform condition tends to saturate when it reaches approximately $1^\circ/\text{s}$. The corresponding gain curves for the *laterally tilted platform* condition, in contrast, resembled those with the stationary platform, although with slightly enhanced gain values (not shown).

Thus, the visually evoked COM excursion showed a pronounced velocity saturation in the form of a hyperbolic decay at $0.1^\circ/\text{s}$ when ankle joint proprioceptive feedback was present on the stationary platform. A similar saturation, but an order of magnitude higher, was found on the BSR platform where the proprioceptive feedback is disabled (hyperbolic decay at $1.0^\circ/\text{s}$). A slight enhancement of the gain of the visual response, which occurred with the laterally tilted platform, remained without major effects on the saturation characteristics.

Gain over stimulus amplitude Reconsider Fig. 4b and note that the left-hand ends of the gain curves for the $\pm 0.25^\circ$ stimulus, the $\pm 0.5^\circ$ stimulus, and so forth, decrease with stimulus amplitude, although they are not yet affected by the velocity saturation. This is similar in Fig. 4a with the much lower gain values for the stationary platform condition. The findings suggest the existence of a displacement saturation in addition to the aforementioned velocity saturation. Indeed, when we plotted gain over peak stimulus amplitude for those trials in which the responses were not affected to a considerable degree by the velocity saturation, the values decreased in a roughly hyperbolic decay. Similar to the velocity saturation, we superimposed calculated COM displacement values on the experimental data for comparison (not shown). The comparison suggested that the visually evoked COM excursion in the BSR platform condition tends to saturate with COM displacements in the range of about $0.5\text{--}1.0^\circ$, whereas the saturation

range was considerably smaller (about $0.1\text{--}0.2^\circ$) in the conditions with both the stationary platform and the laterally tilted platform.

Thus, the visual response appears to be shaped by both a velocity and a displacement saturation (in addition to the frequency effect). The displacement saturation is again smaller with the stationary platform or the laterally tilted platform as compared to the BSR platform condition by almost an order of magnitude.

Statistics

A comparison of response amplitude across the three platform conditions showed that the aforementioned differences were statistically significant ($F=233.2$, $P<0.0001$; factorial ANOVA with the three factors, namely, platform condition, stimulus amplitude and stimulus frequency; the values for stimulus amplitude were $F=13.3$, $P<0.0001$; frequency, $F=35.6$, $P<0.0001$).

Vestibular loss patients

We were interested in how the absence of vestibular input in the patients affects the frequency dependency of the visual response and its velocity and amplitude saturation in the three platform conditions.

Gain over stimulus frequency The average gain and phase curves over frequency of the patients on *stationary platform* are shown in Fig. 3d (missing data for the $\pm 0.25^\circ$ and $\pm 0.5^\circ$ stimuli at 0.4 Hz represent 'falls'; see [Methods](#)). Gain tended to decrease with increasing stimulus frequency (the exception being the gain curve for the $\pm 1^\circ$ stimulus). But this effect was less pronounced than that in the normal subjects. Overall, gain was more than double that of normals (232%, on average), while the phase was similar. The gain curves in the figure also show a decrement with increasing stimulus amplitude, which was somewhat less pronounced than in the normal subjects.

The corresponding plot for the *BSR platform* data are shown in Fig. 3e (missing data because of 'falls': $\pm 4^\circ$ stimulus at 0.2 Hz and 0.4 Hz, $\pm 2^\circ$ stimulus at 0.4 Hz). Noticeably, unlike the earlier case with stationary platform, the gain curves here *increase* with increasing frequency. Yet, the phase is similar as before (showing a slight lead at 0.05–0.2 Hz and a lag at 0.4 Hz) and there is also a gain decrement with increasing stimulus amplitude.

In the experiment with the *laterally tilted platform* (Fig. 3f; note again the different scale on ordinate), the main features of the gain curves were roughly similar to the stationary platform condition (frequency and amplitude dependency). But they showed an increase in gain level by 50% for the $\pm 0.25^\circ$ and $\pm 0.5^\circ$ stimuli, on average.

Thus, patients standing on the stationary platform or the laterally tilted platform showed essentially normal

frequency characteristics of their visual responses, this on an enhanced gain level as compared to the normals. In contrast, clearly abnormal responses were obtained on the BSR platform. The gain increased with increasing frequency, while the phase remained approximately normal. *Gain over stimulus velocity* Figure 4c shows the corresponding replot of the patients' data for the *stationary platform* condition. The gain curves tend to decay with increasing stimulus velocity. The abnormally high gain of patients' responses is reflected by the fact that the curves remain mostly well above the 0.1°/s comparison curve (0.1°/s COM curve). The decay differs from that of the normals in that it is more flat and does not show the hyperbolic form. Similar findings, although with still higher gain and flatter decay, were obtained in the *laterally tilted platform* condition (not shown).

With the *BSR platform*, the patients' gain curves over stimulus velocity (Fig. 4d) showed the opposite of a saturation behaviour. The five curves for the five different stimulus amplitudes *increased* with increasing stimulus velocity. On the other hand, the gain curve for the smallest stimulus amplitude reached the highest values and that for the largest stimulus amplitude the lowest gain values, which again reflects a saturation related to stimulus amplitude. Because peak stimulus velocity increases with peak displacement during sinusoidal stimulation, the aforesaid increase in the gain curves cannot be considered a velocity effect but must mainly represent a frequency effect.

Gain over stimulus amplitude The analysis of gain over stimulus amplitude did not add new aspects and is, therefore, not shown. In the plots for the *stationary platform* and the *laterally tilted platform*, the gain curves showed a weak and relatively flat decay. With the *BSR platform*, the gain curves showed abnormally high values and decreased with increasing stimulus amplitude, but the decay was flat and remained well above the 0.5–1.0° saturation range of normals.

Thus, both with the stationary platform and the laterally tilted platform, patients' visual responses were basically similar to those of the normal subjects, apart from the higher gain values and less-pronounced saturation effects. On the BSR platform, their responses showed an abnormal *increase* in gain with increasing frequency (and, as a secondary, concomitant effect of this, with velocity) and a displacement saturation. In contrast, the phase was essentially normal. We will attribute the abnormal gain increase to a tendency of patients' postural system to show a resonance behaviour in this condition (see [Discussion](#)).

Restriction of visual field size and presentation of 'virtual reality' visual stimulus (normal subjects only)

In the pilot experiments we had learned that a 'virtual reality' visual scene is less powerful than the 'real world' stimulus in evoking a postural response (see [Introduction](#)). We were interested to use the less-effective stim-

ulus for comparison, because we wanted to learn how a weakening of the visual effect affects the saturation characteristics of the response. Since the use of the 'virtual reality' stimulus entails a restriction of the visual field (90°×66°, w×h), we first repeated the above experiments with the 'real world' stimulus using a comparable field restriction. The result was that the gain and phase curves in the three platform conditions showed essentially the same frequency, velocity and amplitude characteristics as before with the full visual field (not shown). Overall, gain level was only slightly reduced: the average values across all stimulus frequencies and amplitudes amounted to 96% with the stationary platform, 88% with the laterally tilted platform and 97% with the BSR platform (respective values for full field: 100%). Statistically, the differences between full versus restricted visual fields were significant ($F=61.2$, $P<0.001$), as ascertained by post hoc analysis ($P<0.001$; Scheffe test).

Before applying the experiment in its full length with the 'virtual reality' stimulus, we tested a shortened version of it with only one stimulus frequency (0.1 Hz). We instructed subjects, as before, to keep their gaze near the centre of the scene and we gave them no further tasks ('*no mental task*' condition). Gain of the visual response decreased to clearly less than half: the average value across all stimulus amplitudes amounted to 27% with the stationary platform, 40% with the laterally tilted platform and 31% with the BSR platform (referred to 'real world' stimulus with restricted field: 100%). Statistically, the differences between 'virtual' versus 'real' visual scene were significant ($F=186.5$, $P<0.0001$), as ascertained by post hoc analysis ($P<0.0001$; Scheffe test). We considered the visual effect in this condition as too weak for the intended comparison.

We, therefore, combined the virtual reality stimulus in the final experiment with a mental task, having observed in pilot experiments that this task enhances the visual effect to some extent. Subjects were instructed to focus visual attention on a moving disc in the 'virtual reality' scene in front of them and to read aloud varying sequences of numbers that were presented to them on the disk ('*mental task*' condition; see [Methods](#)). With this task, the complete sets of trials were repeated, using the same stimulus amplitudes (0.25°–4°) and frequencies (0.05–0.4 Hz) as before. Overall, gain of the visual response (referred to the 'real world' stimulus with restricted field: 100%) was reduced to approximately half: the average values across all stimulus amplitudes and frequencies amounted to 46% with the stationary platform, 59% with the laterally tilted platform and 50% with the BSR platform. Statistically, the differences between 'virtual' versus 'real' visual scenes were significant ($F=248.5$, $P<0.0001$), as ascertained by post hoc analysis ($P<0.0001$; Scheffe test). Despite the gain reduction, the gain curves over stimulus frequency, velocity and amplitude showed similar characteristics as before with the 'real world' stimulus (not shown). This applied to all three platform conditions (stationary, laterally tilted, BSR).

Thus, weakening the visual effect by presenting a ‘virtual reality’ instead of a ‘real world’ visual stimulus had no considerable effect on the saturation (and frequency) characteristics of the responses. As a reminder, when subjects in the previous experiments were standing on the laterally tilted platform the visual effect became stronger (also with essentially unchanged saturation and frequency characteristics). One would therefore expect for the ‘virtual reality’ experiment that the gain reduction, seen with stationary platform, becomes partially reversed with the laterally tilted platform. This prediction was confirmed in the corresponding trials.

Perception of scene motion

Even the smallest visual stimulus in our experiments (peak amplitude, 0.25° ; peak velocity, $0.08^\circ/\text{s}$) evoked a clear postural response, at least in the averaged data. Yet, the majority of our subjects experienced the scene always as stationary with the smallest stimulus, a finding that might suggest a higher detection threshold for conscious perception than for postural control. From another view point, one could argue that the occurrence of the postural response is related to subjects’ conjecture that the scene is not moving, but represents a stationary space reference for the orientation of the body. In this view, one could also try to relate the observed velocity and amplitude saturation of the visual response to the detection of scene motion. These considerations led us to obtain an estimate of our subjects’ detection threshold of the visual motion stimulus for comparison with the corresponding literature and the present postural data. To this end, we asked the subjects after each trial to judge the scene as “clearly moving” or “stationary” (being aware of the fact that the overall experimental design without sham trials invoked a bias towards the “moving” judgement).

Percentage of perceiving the scene as moving varied with stimulus frequency and amplitude. With the full field ‘real world’ visual stimulus and the platform stationary, all subjects (100%) experienced the scene as moving with all five stimulus amplitudes (± 0.25 , 0.5 , 1 , 2 and 4°) at 0.4 Hz, with the four largest stimuli at 0.2 Hz and with the three largest stimuli at 0.1 and 0.05 Hz (when plotted over stimulus velocity, the 100% value applied to the range of 0.63 – $2.51^\circ/\text{s}$). Below these ranges, the percentage decreased, reaching 37.5% with the smallest and slowest stimulus (0.25° at 0.05 Hz). In the plot over stimulus velocity, the $> 50\%$ value ($>$ chance level) was reached with $0.31^\circ/\text{s}$, which we took as the detection threshold. With the other two platform conditions, the distributions of the percentage values over frequency, amplitude and velocity were similar (and the $> 50\%$ value was again reached with $0.31^\circ/\text{s}$ peak stimulus velocity). In the experiments with the ‘virtual reality’ scene with ‘mental task’, the percentage values tended to be clearly lower. For instance, the 100% level was reached with the 2° and 4° stimuli at 0.2 Hz and the

1° , 2° and 4° stimuli at 0.4 Hz. In terms of peak velocity, the $< 50\%$ value (presumed threshold) was reached with the $1.3^\circ/\text{s}$ stimulus.

The findings suggest that the detection threshold for consciously perceiving the visual motion stimulus is higher than that for posture control (the latter appears to be almost inexistent). Furthermore, in the individual case, the occurrence of the postural response was not related to a conjecture by the subject that the scene is stationary in space. On the other hand, in the averaged data for the ‘real world’ stimulus and the stationary platform, the presumed threshold for detecting the visual motion ($0.31^\circ/\text{s}$) was in the order of magnitude of the curtailment of COM excursion ($0.1^\circ/\text{s}$). However, such a correspondence did not hold in the BSR platform condition, since the threshold was the same ($0.31^\circ/\text{s}$), whereas the curtailment of the COM excursion was one order of magnitude higher ($1^\circ/\text{s}$).

Discussion

The postural response to visual stimulation of our subjects showed pronounced frequency and saturation effects, a finding that is in line with previous work in the literature (see [Introduction](#)). The effects of frequency could be discerned from those of saturation, in that the frequency-induced gain changes are associated with phase changes unlike the gain changes induced by saturation. We attributed the frequency effects mainly to the dynamics of the postural system as a whole (i.e. including biomechanics and physics) rather than to transfer characteristics of the visual system (see below). As for the main focus of our study, the saturation, we observed two effects, one related to stimulus velocity and the other to displacement.

In the following discussion we proceed from the aforementioned notion that saturation mainly stems from the interaction between the visual response and other sensory cues. In this view, the visually evoked body excursion activates vestibular and proprioceptive cues, which in their part try to maintain body uprightness and, thereby, would counteract the visual response. The counteraction itself would only weaken the visual responses, however. It must also show non-linear properties (e.g., in terms of a vestibular or proprioceptive threshold) in order to lead to saturation. Since detection thresholds of the vestibular and proprioceptive systems are known in the psychophysical literature, we asked whether the postural findings can be related somehow to the perceptual thresholds. Furthermore, we used vestibular and proprioceptive thresholds in a previous postural control model to explain non-linearities of the responses to pull and tilt stimuli (Mergner et al. 2003; Fig. 5). We will therefore consider this model also.

We start our considerations with the four different sensory conditions used (proprioceptive cues present/absent, vestibular cues present/absent), before examining the effects of a gain modification of the visual signal

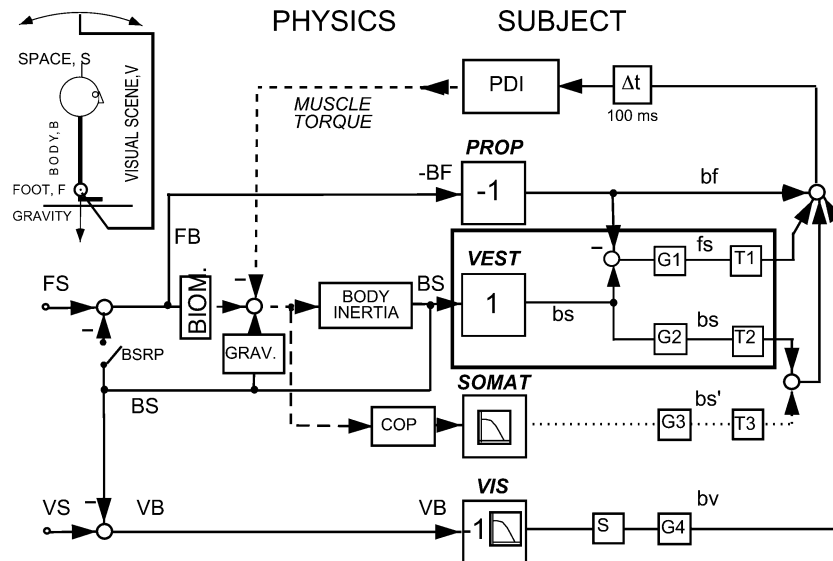


Fig. 5 Multisensory model of posture control of Mergner et al. (2003). Details are described in Appendix. *Inset on top left* defines 'PHYSICS' part: a one-segment body (including head, trunk and legs) pivots in the sagittal plane as an inverted pendulum about the ankle joint on a potentially tilting platform with a rotating visual scene representing the external stimulus (all rotation axes through ankle joint). *FS* foot-in-space angle (resulting from platform tilt); *FB* foot-to-body angle (equal to $-BF$); *BS* body-in-space angle; *VS/VB* angle of visual scene in space/to body. Open switch *BSRP* mimics body sway referenced platform. Box *BIOM* (biomechanics) transforms *FB* into ankle torque. The subjects' anthropometric parameters are contained in the boxes 'BODY INERTIA' and 'GRAVITY'. Torque at the ankle joint leads to shift of the centre of pressure (box *COP*). *Dashed lines* represent torque and *solid lines* angles. 'SUBJECT' part of model (*on the right*): Boxes *PROP*, *VEST*, *SOMAT* and *VIS* represent the proprioceptive, vestibular, plantar pressure (somatosensory) and visual sensors, respectively (*SOMAT* and *VIS* show low-pass filter properties, as indicated by symbols in these boxes). *bf*, *bs*, *fs* and *bv* are internal representations of *BF*, *BS*, *FS* and $-VB$, respectively (*bs'*, a *bs* estimate derived from *SOMAT*, is used instead of signal *bs* by patients as well as by normals on *BSR* platform). Elements contained in the *dark grey box* were omitted when simulating the patients. *T1*, *T2* and *T3*, detection thresholds; *G1*, *G2* and *G3*, fixed gain values (see Fig. 7); *G4*, gain of the visual signal, adjusted to fit simulated with experimental data; *S* saturation element. All delays in the system are represented as one dead time ($\Delta t = 100$ ms). Box *PDI* represents neural controller with proportional, differential and integrative factors (normals: 12.2 Nm° , 4.4 Nms° and 1.6 Nm/s° ; patients: 15.7 Nm° , 5.2 Nms° and 1.6 Nm/s° , respectively)

(induced by the 'virtual reality' stimulus and the laterally tilted platform). Therewith, we refer to our model but explain only its most relevant features leaving a detailed description of it to the Appendix. A major function of the model is to create, by way of intersensory interactions, internal representations of the external stimuli. A consequence is that the model's sensory feedback changes 'automatically' when the stimuli in the environment change (see also Mergner 2004). This allows us to simplify the model for each of the two environmental situations used (stationary/*BSR* platform) by removing the inactive parts. Further simplified versions resulted when we mimicked the loss of vestibular function by

removing the vestibular sensor from the model. This yielded four simple models, one for each of the four sensory conditions (Fig. 7a–d).

Visual response with both proprioceptive and vestibular cues present (normal subjects, stationary platform)

The visual responses were smallest with normal subjects on the stationary platform. As mentioned before, they saturated in two ways. One was a saturation with increasing stimulus velocity. In the corresponding gain plots, the curves showed an essentially hyperbolic decay with increasing stimulus velocity, reflecting a curtailment of COM excursion when peak COM velocity exceeds a 'threshold' of $0.1\text{--}0.2^\circ/\text{s}$ (compare $0.1^\circ/\text{s}$ dotted curve in Fig. 4a). The other was a saturation which we related to COM displacement (at $0.1\text{--}0.2^\circ$). One tends to attribute these saturation effects mainly to the ankle joint proprioceptive feedback because they dramatically changed when this feedback was disabled (*BSR* platform; see below).

Interestingly, Fitzpatrick and McCloskey (1994) reported in a psychophysical study that conscious self-motion perception during stance of normal subjects on stationary support is determined primarily by leg proprioception. They came to this conclusion on the basis of detection threshold measurements. They reported velocity and displacement thresholds for leg proprioception of approximately $0.1^\circ/\text{s}$ and 0.1° , respectively, which is in the same order of magnitude as the above saturation values. We take this correspondence as indicating a meaningful congruency between action (here, posture control) and perception. But there appears to be no simple and straightforward way to relate the two phenomena to each other, as we will see in the following with the model simulations.

When simulating (in a previous study) human proprioception in a simple feed forward model of self-

motion perception, we could directly implement the perceptual threshold; the model's output then reflected the threshold effects which we had obtained experimentally with monomodal stimulation and appropriate instructions to the subjects (Mergner et al. 1991). The situation with the postural control mechanism is more complicated. It involves not only a motor system but also a sensory feedback, and this from several sensors. In fact, in our posture model (Fig. 7a), we assume feedback from four sensory systems: the visual, leg proprioceptive, vestibular and somatosensory systems (boxes *VIS*, *PROP*, *VEST* and *SOMAT*, yielding internal representations of the a-p angular excursions between visual scene and body, body and foot support, and body in space, and of the a-p shifts of plantar sole reaction forces, respectively). Since here *SOMAT* is not contributing to the feedback in this condition (see Appendix), there remain inputs via the *VIS*, *PROP* and *VEST* systems. These signals are combined at an internal summing junction for the presumed feedback control. Since the original model did not include a *VIS* system, we added it here for the present experiments (without yet assuming visual interactions with the other cues at sensory levels; see below).

We found that our model is able to mimic the visual responses obtained in the present study. In the model simulations, we addressed the following four points:

Gain adjustment of visual signal

Application of the model to the present experiments required that we adjusted the gain of the internal visual signal in the model for each experimental condition separately, thereby trying to fit the simulation data to the experimental data. A successful fit would allow us to obtain an estimate of how the internal visual signal is modified within the postural control system.

In the simulations, the model's output (BS, body in space) was compared to the visual stimulus (input VS, visual scene in space) for different adjustments of *VIS* gain (box G4). We found that the simulation data became similar to the experimental data when the gain was set to a very low value (0.05). The corresponding plot of BS gain over stimulus velocity is shown in Fig. 6a (together with the calculated $0.1^\circ/\text{s}$ dotted BS curve, to ease comparison with the experimental data in Fig. 4a). Note the hyperbolic decay in the simulated gain curves, which mimics quite well the measured one in the experimental data. Also, the decrement of the initial parts of the gain curves with increasing stimulus amplitude, i.e. the amplitude saturation, is mimicked. Using an automated optimisation of the visual path's parameters, the fit between simulated and experimental data became only slightly better (see Appendix). The low visual gain indicates that the visual signal is largely suppressed in

Fig. 6 Simulation results obtained with the model in Fig. 5. Presentation is analogous to that in Fig. 4 (COM gain over stimulus velocity). **a, b** Simulation results for normal subjects. **c, d** Vestibular loss patients. **a, c** Stationary platform. **b, d** 'Body sway referenced', BSR platform. Note different scales on ordinates

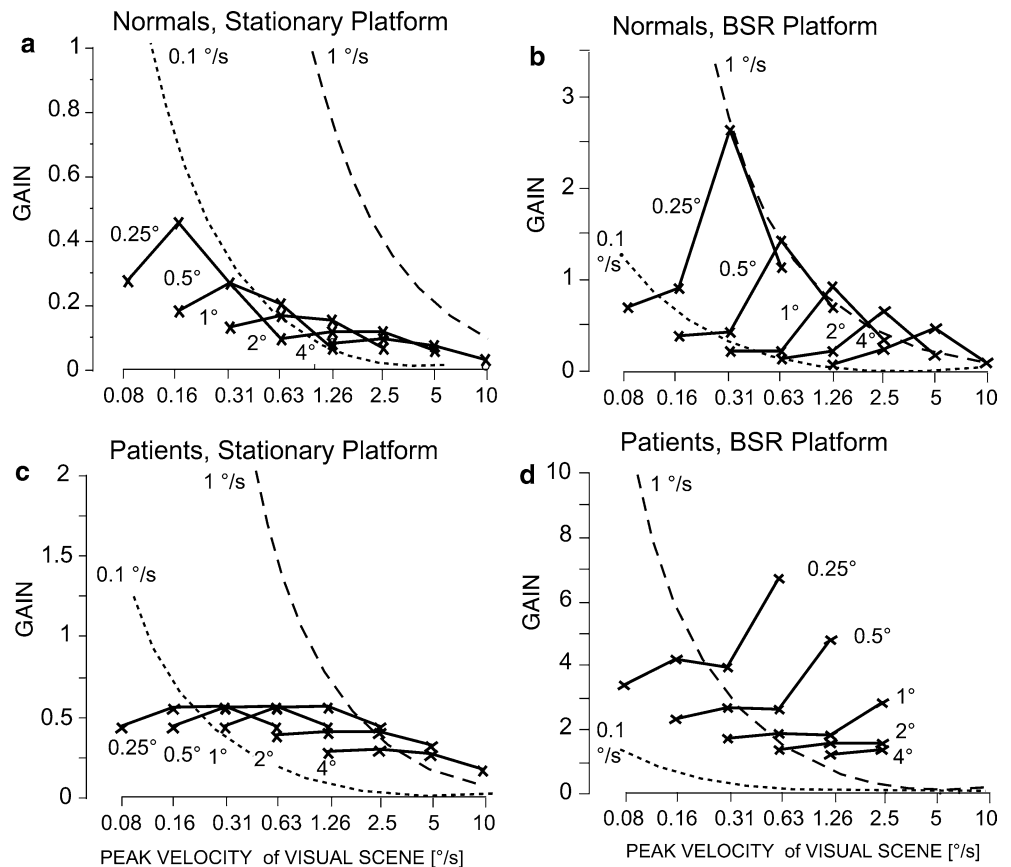
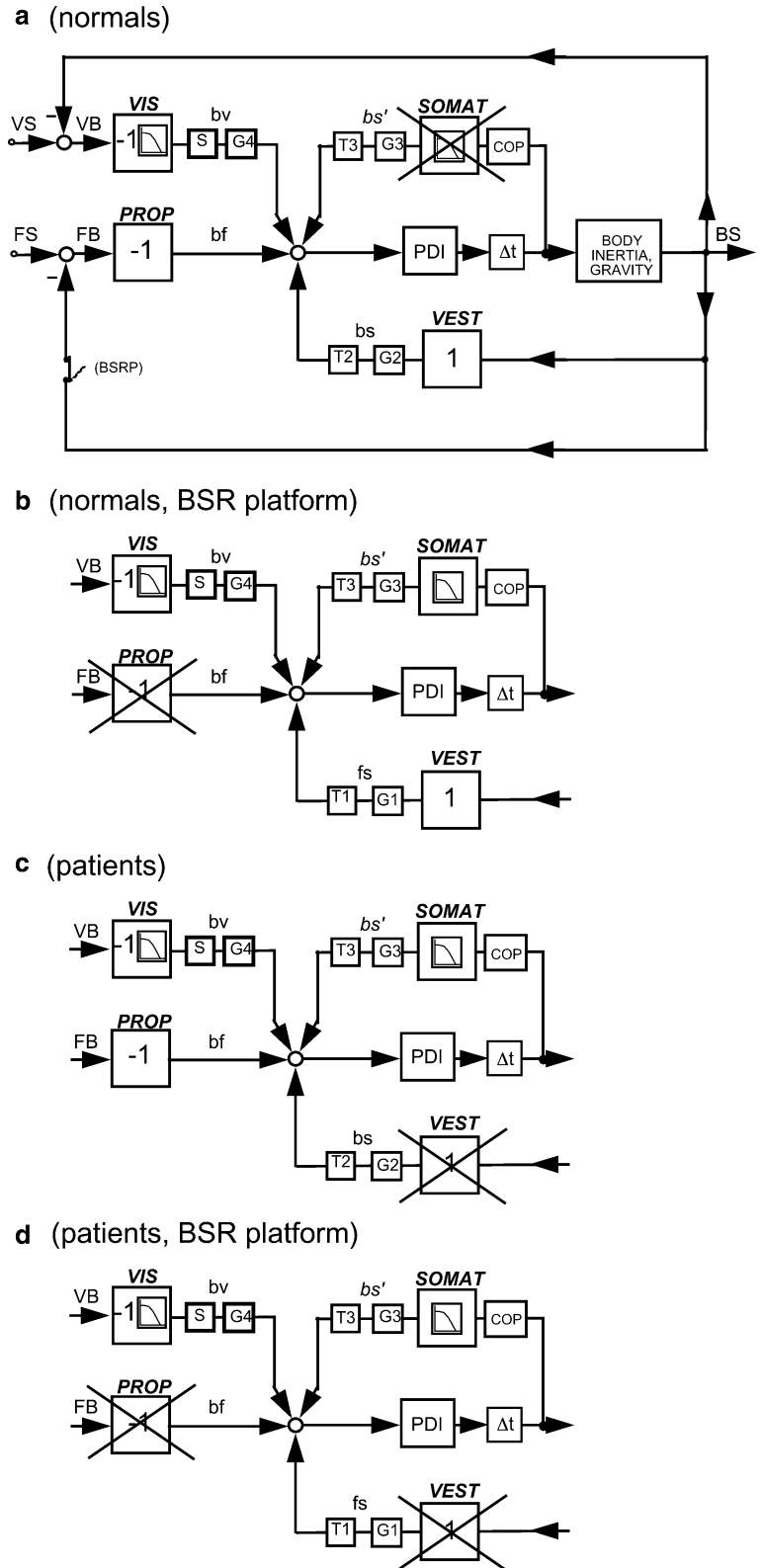


Fig. 7 Simplified versions of the model shown in Fig. 5, which result when it is applied to the four sensory conditions used (a–d). For abbreviations, see Fig. 5. **a** Normal subjects, stationary platform. Sensory feedback occurs via the sensors *PROP*, *VEST* and *VIS*, whereas the plantar pressure cues are not used here (crossed box *SOMAT*). Furthermore, the internal representation of FS, signal fs, is omitted, because $FS = 0^\circ$ (stationary platform). Gain G_4 of the visual path was varied to fit simulated to experimental data (see *Discussion*). S velocity saturation, $3.0^\circ/s$. **b** Normal subjects, BSR platform. Proprioceptive feedback is disabled (crossed box *PROP*) and motion of platform is registered via vestibular path that yields fs. The vestibular signal bs is replaced by the bs' signal from *SOMAT*. **c** Vestibular loss patients, stationary platform. With loss of vestibular input (crossed box *VEST*) signal bs' from *SOMAT* substitutes bs. Otherwise as in **a**. **d** Patients, BSR platform. As in **c**, but in addition to the vestibular loss the proprioceptive feedback is disabled. Low-pass filters of *SOMAT* and *VIS* are first order with corner frequencies of 0.5 and 0.8 Hz, respectively. Further details in Appendix. List of gain and threshold values: $G_1 = 0.7$, $T_1 = 0.1^\circ/s$; $G_2 = 0.9$, $T_2 = 0.06^\circ$; $G_3 = 0.8$, $T_3 = 0.06^\circ$



this condition, compatible with earlier findings of Peterka (2002). As will be discussed further later, we attribute this suppression to a visual-vestibular interaction at sensory levels.

Saturation of visual signal

To what extent can the saturation element in the visual path, which we implemented in analogy to the known

saturation in the optokinetic pathway (see [Introduction](#)), explain the saturation of the visual response? In the simulations, we found that the velocity saturation in the visual path (S) makes only a very small contribution as compared to the threshold effects that we describe in the following paragraph.

Thresholds of non-visual signals

How to explain the apparent correspondence between the saturation characteristics in the postural data and the psychophysical thresholds? Note that the *PROP* pathway of the model contains no thresholds. We explored these issues in two ways:

1. When we removed the only threshold contained in the model of Fig. 7a, i.e. a position threshold in the vestibular path ($T_2=0.06^\circ$), both the velocity and displacement saturation effects in the simulation responses were eliminated (apart from a small remnant due to the saturation element S in the visual path, see above). Noticeably, the velocity saturation effect in the simulation resulted from a combination of the position threshold and the frequency effects in the model. Thus, our postural control model mimics the saturation characteristics of the experimental data without explicitly containing a $0.1^\circ/\text{s}$ velocity threshold and a 0.1° position threshold.
2. The model could be transformed into one with proprioceptive feedback alone and with both a $0.1^\circ/\text{s}$ and a 0.1° threshold, while maintaining essentially the same simulation results as before. Note that both the vestibular signal and the proprioceptive signal in the model register body motion with respect to the stationary support so that the vestibular feedback can be substituted by proprioception. This could be done in different ways, either by simply exchanging the sensor and leaving the aforementioned position threshold in the now proprioceptive path (no velocity threshold) or by replacing this single threshold by an in-series combination of the psychophysical $0.1^\circ/\text{s}$ velocity threshold and 0.1° position threshold (which required a gain adjustment of the path), or by adding two proprioceptive paths, one for each of the two thresholds. Thus, it was possible to create, for comparison with the psychophysical studies in which proprioception was tested selectively, a monomodal proprioceptive posture model which contains the psychophysical thresholds exactly and still shows the above saturation characteristics.

Given that a control mechanism such as the proprioceptive model exists, what could be the functional significance of parallel proprioceptive pathways? We deem it possible that conscious proprioception at high processing levels (cognitive levels), which carries the perceptual thresholds, can help the proprioceptive path at low levels, in substitution of vestibular feedback during postural control on stationary platform. There

might even be separate proprioceptive channels for velocity and position, a notion to be elaborated in a future study. This view is rather speculative, admittedly. The main point we want to make here is that the functional equivalence between the original model and the monomodal proprioceptive model lends support to the assumption of an action-perception congruency. Yet, it is to denote that the proprioceptive model would fail when the environmental situation is changed into one with moving platform (since it tries to stabilise the body with respect to the platform and not in space), whereas the model in its original form (Fig. 5) copes with such a change.

Threshold of visual signal

How does the detection threshold for consciously perceiving motion of the visual scene, which we obtained from our normal subjects in the present experiment, fit into this picture? The value obtained ($0.3^\circ/\text{s}$) is well in line with the literature (Fitzpatrick and McCloskey 1994; $0.1\text{--}0.3^\circ/\text{s}$). As already mentioned in Results, the threshold value is only slightly higher than that of the COM curtailment of the postural response ($0.1^\circ/\text{s}$), so that one may tend to assume a direct relationship between the two phenomena. However, this assumption appears not to hold, since, in the BSR platform condition, the threshold was the same, whereas the COM curtailment occurred at a much higher value ($1^\circ/\text{s}$).

When we implemented this psychophysical threshold into the visual path of the posture model, its output BS conceivably became zero with slow stimuli, which is unlike in our experiments. However, such a threshold must not necessarily represent a problem for the posture control system. In the simulations, the problem could be overcome by having, in addition, a visual path with no considerable threshold (an approach analogous to the one just described above with proprioception) or by internally adding white noise at the sensory signals' summing junction. Experimental evidence for a relationship between detection thresholds and internal noise in the human spatial orientations system has been reported in a recent psychophysical study (Mergner et al. 2001).

Proprioceptive cues absent and vestibular cues present (normal subjects, BSR platform)

Our normal subjects showed much larger visual responses on the BSR platform than on the stationary platform. Especially with small visual stimuli, the body excursions could by far exceed the visual scene excursions. Saturation occurred again in two ways, i.e. with increasing stimulus velocity (hyperbolic decay in Fig. 4b) and with increasing stimulus displacement (decrement of the initial parts of the gain curves in Fig. 4b). Also, similar to before, the saturation effects

occurred when the visually evoked COM excursion reached certain velocity and displacement values. But these values were an order of magnitude higher ($\approx 1^\circ/s$ and 1° , respectively). Since ankle joint proprioceptive feedback was disabled in this condition one would tend to attribute these effects mainly to vestibular mechanisms.

In the psychophysical study of Fitzpatrick and McCloskey (1994), the values for the vestibular velocity and position thresholds during stance were about a magnitude higher than for the leg proprioceptive ones ($\approx 1^\circ/s$ and 1° , respectively). A $1^\circ/s$ vestibular threshold was also reported for the conscious self-motion perception in the horizontal rotational plane (Benson et al. 1989; Mergner et al. 1991). Thus, action-perception congruency appears to apply here also.

Again we tried to mimic the postural data by the model simulations. The model for this sensory condition is shown in Fig. 7b (disabling the proprioceptive feedback refers to opening the switch BSRP in Fig. 7a). Motion of the platform, resulting from its coupling to the body excursion, is now thought to activate a *VEST* system which is different from the one in Fig. 7a in that it shows a velocity threshold ($T1 = 0.1^\circ/s$) and a different gain ($G1$; see Appendix). Furthermore, the model involves the *SOMAT* system. With the visual gain adjusted to 0.05 as before, the simulation data well mimicked the experimental data with both a velocity and a displacement saturation (Fig. 6b). Optimisation of the visual path slightly improved the data fit with a somewhat increased visual gain (0.33) under retention of the saturation characteristics. When we removed the two thresholds in the model (*VEST*, $0.06^\circ/s$; *SOMAT*, 0.06°), the saturation effects of the visual responses were essentially abolished. Thus, also in this condition, our postural control model mimics the saturation characteristics of the experimental data without explicitly containing a vestibular $1^\circ/s$ velocity threshold and 0.1° position threshold.

How do the model simulations relate to the psychophysical findings of $1^\circ/s$ and 1° vestibular thresholds? Although there is no direct relationship between the psychophysical thresholds and the thresholds in the model, we could establish a bridge between the two. We did so by creating a version of the model in which we made the vestibular cues the only non-visual feedback (an approach that we considered appropriate for comparison with a psychophysical condition in which vestibular cues were tested selectively). This was achieved in a way analogous to before by replacing the *SOMAT* feedback with vestibular feedback. For the replacement we used two vestibular paths, one with a $1^\circ/s$ and the other with a 1° threshold. The functional equivalence between this monomodal vestibular model and the original one again lends support to the assumption of an action-perception congruency.

A further question which we tried to answer with the help of the model simulations is: how to explain the large gain values in this condition? We inspected the single

response traces of the simulations and found that the responses were characterised by large body oscillations in the low-frequency range (0.1–0.3 Hz). Similar oscillations also occurred intermittently in our experimental data and have been documented in the study of Peterka and Loughlin (2004) for this condition. They represent a tendency of the feedback system to show a low-frequency (0.1 Hz) resonance behaviour when the loop gain is low (compare Peterka 2001). Why would the loop gain here be low? Noting that the resonance behaviour was prominent with small stimuli, we tend to relate the low loop gain in this condition to the thresholds, at least in part (the thresholds suppress part of the sensory feedback and this is relatively more for small stimuli than for large stimuli).

Vestibular cues absent and proprioceptive cues present (patients, stationary platform)

The responses of the patients in this condition were basically similar to those of the normal subjects. Obviously, patients noticed, although not necessarily consciously, that it was the platform which was stationary (and suitable for use as a space reference) and not the visual scene. They likely did so because there were no changes in the ground reaction force under their feet (no *SOMAT* signals) that were directly related to the relative motion between scene and body. Yet, the patients' gain of the visual responses was somewhat larger than that of the normal subjects, while the phase was essentially normal. Furthermore, the decay of gain with increasing stimulus velocity and displacement was less steep than in normals. Because we do not know of comparable psychophysical threshold data from vestibular loss patients in the literature, we restrict our further considerations to a comparison with the simulated data.

The model for the patients on the stationary platform (Fig. 7c) contains, in addition to the *PROP* system, a *SOMAT* system (compare Appendix). When we adjusted, in a first step, the visual gain to a value of 0.2, the simulation data including the saturation effects (Fig. 6c) rather well mimicked the experimental data (compare Fig. 4c). The automatic optimisation of the visual path parameters improved the fit slightly with a visual gain of 0.4. In the simulations, the reduced slope of the velocity saturation mainly stemmed from the increase in visual gain. The saturation effects were primarily caused by the position threshold in the *SOMAT* path (0.06°). Modifications of the model were not tested.

Vestibular and proprioceptive cues absent (patients, BSR platform)

It may appear surprising that the patients were able to stabilise their bodies on the almost continuously moving platform (it was moving 1:1 with their body sways). The first reason for surprise is that the patients

were able to cope with the unusual way of balancing in this condition. Intuitively, we tend to relate a ‘body righting in space’ to a corresponding adjustment of ankle joint angle (body-to-foot), given that we know the foot support angle in space. In the BSR platform condition, however, equilibrium control requires an adjustment of ankle torque, without this producing a concomitant change in ankle angle. Second, one may wonder how the patients were able to cope with the fact that not only was the scene moving, but also the platform. The explanation would be that patients used the scene as a space reference for their posture control (and needed to do so, because when tested with eyes closed, they always tended to fall). We deem it likely that they could achieve body equilibrium because the scene excursions used were rather small ($\leq 4^\circ$). But it turned out to be also important that these excursions were rather slow, because patients fell with faster excursions ($> 2.5^\circ/\text{s}$), and this even if they were rather small ($< 1^\circ$; compare Fig. 4d).

The frequency characteristics of patients’ visual response in this condition were quite abnormal. The phase showed essentially a normal lag with increasing frequency, but gain showed an *increase*. There was also a gain increase with stimulus velocity, but this reflects primarily the frequency effect. The reason for this assumption is that the increase in stimulus amplitude, which equally increases stimulus velocity with the sinusoidal stimulation, led to a decrease in gain. We tried to understand better the effects with the help of our model simulations.

The model for the BSR platform condition is shown in Fig. 7d. It contains the *SOMAT* path with the 0.06° threshold, as before, but no longer the *PROP* feedback. A good fit between simulated and experimental data was achieved when visual gain was adjusted to 0.7 (a value ≥ 0.4 was required for body stability; the procedure for the optimal fit yielded a value of 0.53). Removal of the threshold in the *SOMAT* path almost completely eliminated the amplitude saturation, while the gain still increased with increasing frequency, albeit to clearly lower values. Inspection of the individual simulation responses revealed a tendency for body oscillations in the range of 0.5–1.0 Hz, which also could be found in the experimental data. It is known that a tendency for high-frequency resonance in the postural loop can occur with high loop gain leading to abnormally large and fast body excursions (Peterka 2000; Peterka and Loughlin 2004; Maurer et al. 2004). In the situation considered here, however, mainly other factors contribute to the oscillatory behaviour (the presence of two mutually competing references with similar gain, represented by the signal from the *SOMAT* path for stabilisation in space versus the signal of the visual path for stabilisation with respect to the moving scene; low-pass filters in the two paths and a threshold in the *SOMAT* path). Thus, the simulations helped us to explain the abnormal postural responses and the instability of the patients in the BSR platform condition.

Previous studies of Peterka and Benolken (1995) and Peterka (2002) reported visual postural responses with frequency and saturation characteristics similar to the ones described here. Also, the weighting factors of the visual signal that Peterka (2002) calculated from his data for the visual responses of normals and patients are similar to the gain values we found in the present study. But these earlier studies did not distinguish between velocity and displacement saturation and they did not aim to elucidate the mechanism underlying the saturation. Furthermore, although the authors of the previous studies noted some similarity between their postural data and perceptual threshold data in the literature, they did not elaborate on this point. Instead, they related the saturation to a still-to-be-defined ‘sensory weighting’ mechanism. Finally, the previous studies did not find considerable saturation in vestibular loss patients on the BSR platform, which is different from the present findings. We would tend to relate this difference to the fact that their patients had lost vestibular function during late adulthood, while the loss in our patients occurred in childhood, so they may have adapted better.

Weighting of sensory cues, performed in an adaptive way based on the noise in the sensory signals, is a key feature of the posture control model of van der Kooij et al. (2001). Interestingly, although no threshold mechanisms were implemented in their model, the responses obtained during simulation showed threshold and saturation characteristics. It remains to be shown to what extent their model is functionally equivalent to our model, but we would like to point out the following difference: our model uses linear inter-sensory interactions to yield a “sensory weighting” that depends on the presence or absence of external stimuli, with the threshold mechanisms which we presume contributing to the weighting (see also Appendix).

As mentioned before, we have not yet implemented a visual interaction with other sensory signals at the internal sensory processing level of our model. The estimates of the visual gain that we obtained in the present study for the four sensory conditions which we used will help us to design such an interaction mechanism in the future. In the previous psychophysical work we have already presented a model that describes the visual-vestibular interaction for human self-motion perception (Mergner et al. 2000a). In this psychophysical model, the visual cues dominate whenever the visual scene is stationary (i.e. a stationary visual scene is taken as space reference for self-motion perception), while they become largely suppressed and the vestibular cues prevail when the scene is moving. We conceive that a functionally equivalent visual-vestibular interaction occurs in the postural control system and is responsible for the suppression of the visual signal when a moving visual scene is presented as stimulus.

Given our assumption that the thresholds in the postural control mechanism are, at least in part, independent of sensory weighting mechanisms, the question arises as to their functional significance otherwise.

Noticeably, these thresholds are thought to reside centrally, i.e. they are distinct from the peripheral detection thresholds of the sensors. In the previous work on perception, we considered them as central mechanisms which suppress internal signal noise with the aim of perceptual stabilisation (Mergner et al. 1991, 2001; in the same token, they may suppress signal drifts which arise, for instance, if internally a position signal is derived from a velocity signal that carries an offset). In the postural control system, however, a ‘noisy’ output in terms of spontaneous sway appears to be desirable for many reasons. To give an intuitive example: attempting to stand absolutely motionless soon becomes uncomfortable and even painful, but maintaining a relaxed stance with ample sway remains comfortable. How is it possible that the thresholds do not suppress the spontaneous postural sway?

One answer to this question would be that, conceivably, centrally arising noise downstream from the thresholds represents a ‘set point signal’ for the controller and thus affects the output. On the other hand, noise arising in the periphery or in the sensory systems tends to be suppressed by the envisaged thresholds. This point, though, has two noteworthy aspects which may compete with each other. First, the noise may help sensory stimulus signals to surpass the thresholds (see above). Second, external stimuli such as gravitational acceleration are responded to by the system only to the extent that they exceed the thresholds (thus, body excursions in response to external forces are not countered by the control system unless they exceed the threshold, by which a kind of ‘discrete’ feedback control could result). Overall, the effects of the thresholds appear to be rather complex and their role for the occurrence of spontaneous sway still remains to be determined. Experimentally, at least, the threshold effects can be assessed rather well, as we have shown here, although their interpretation is more difficult than we anticipated.

Modification of visual signal gain

As mentioned in the Introduction, pilot experiments suggested that the strength of the visual effect depends not only on frequency, amplitude and velocity of the visual stimulus and on the intersensory interactions above considered but also on factors that are yet to be defined in the following. When we presented a ‘virtual reality’ stimulus instead of the ‘real world’ stimulus, the gain clearly decreased. On the other hand, it increased when we superimposed small lateral platform tilts on the a–p visual stimulus. These effects were confirmed and quantified in our final study. Interestingly, other changes of the stimulus presentation were less effective. For instance, reduction of the size of the visual field affected the gain only to a minor degree (see [Results](#)). We would expect the same for a reduction in contrast and/or luminance level of the

visual stimulus, a notion that we have not quantified in this study, but which we have drawn from previous work on self-motion perception (Mergner et al. 2000b).

The gain changes of the visual responses observed with the ‘virtual reality’ scene and the laterally tilted platform appear mainly due to a modulation of the visual signal at input levels. To test this hypothesis, we performed model simulations comparing the effects of such gain changes in the simulations with those obtained experimentally. When we either decreased the gain of the visual signal to 0.01 (from 0.05) or increased it to 0.1 in the model of normal subjects on the stationary platform, gain of the visual response was changed accordingly without major effects on the saturation characteristics, similar to the experimental data (analogous findings were obtained for the BSR platform condition). However, when we increased the gain further up to 0.4, the curves of response gain over stimulus velocity increased and the decay became less steep. Consequently, the gain curves resembled those of the patients on the stationary platform (see above). We take these findings as further support for the descriptive and predictive power of our model.

We assume that the gain changes of the visual signal were caused mainly by cognitive mechanisms. In the condition with superimposed lateral platform tilts, we assume that the tilts interfered with subjects’ notion of a stationary body support. Although not destabilising their body posture to a considerable degree, the tilts likely increased the subjects’ tendency to rely their posture control on the visual scene as a space reference. We assume that this increased the gain of the visual signal. With the ‘virtual reality’ scene, on the other hand, we explain the gain decrease of the visual signal by assuming that the subjects experienced the stimulus as less ‘convincing’ than the ‘real world’ stimulus. We expect that the cognitive effects take place at those sensory processing levels where the visual-vestibular interaction takes place.

The findings obtained with the ‘virtual reality’ stimulus are of general relevance, because this sort of stimulus is being used more and more, not only in research of posture control (e.g., Kuno et al. 1999; Keshner and Kenyon 2000; Akiduki et al. 2003; Tossavainen et al. 2003), but also in video games, motion simulations, etc. As mentioned before, restriction of the visual field size (e.g., by a ‘virtual reality’ set up), reduces the visual response only to a minor degree. The cognitive effects appear to be more relevant. They can likely be related to a number of technical factors that betray the unrealistic character of the stimulus (pixel size, lines of display, unrealistic motion parallax depending on distance of eye fixation point, etc.) and to the a priori knowledge of its illusory character. However, we would also like to point out the advantage of this technology. It allowed us to modify the visual stimulus with little effort such that we could add a mental task (‘mental task’ condition) and thereby bind the subjects’ gaze and visual attention.

Conclusions

In our experiments, we used the motion of a visual scene to evoke postural responses. These visual responses are characterised by saturation. In normal subjects, the saturation occurs with both increasing stimulus velocity and displacement. It shows up rather abruptly when the visually evoked body excursions reach certain velocity and displacement values. These body excursion limits are low with stance on a stationary platform ($0.1^\circ/\text{s}$ and 0.1° , respectively). Very similar values are reported in the psychophysical literature for the velocity and displacement detection thresholds of leg proprioceptive perception. On the other hand, with stance on a BSR platform, a situation where proprioceptive feedback is disabled and vestibular cues are thought to play the major role, analogous saturation characteristics of the visual postural responses are found, but they are one order of magnitude higher ($1^\circ/\text{s}$ and 1°). Again, there appears to be a correspondence with the psychophysical literature which reports very similar values for the vestibular perception thresholds. How can the postural findings be explained and how can they be related to the psychophysical data?

To answer these questions, we performed simulations of the experiments with the help of a posture control model. The model had previously been designed to describe non-linear responses to body pull and support surface tilt stimuli with the help of threshold mechanisms. A visual path was added to the model and the internal visual gain was adjusted for the best fits between simulated and experimental data. The fits were obtained when the visual gain was set at low values (true for normals on the stationary platform and the BSR platform; thus, normals appear largely to suppress the visual input in these experimental situations). The simulation data then showed saturation characteristics which were very similar to those in the experimental data. This applied although the thresholds in the model were much lower than the psychophysical ones and the sensory feedback was not unimodal (the model version for the stationary platform condition contained in addition to proprioceptive cues vestibular cues, and for the BSR platform condition it contained in addition to vestibular cues plantar pressure cues).

We were able to transform the model into a functionally equivalent version with monomodal proprioceptive feedback and the psychophysical thresholds ($0.1^\circ/\text{s}$ and 0.1°) for the stationary platform condition as well as with monomodal vestibular feedback and $1^\circ/\text{s}$ and 1° thresholds for the BSR platform conditions. We speculate that such mechanisms may be invoked in certain situations of the posture control repertoire, when one has to involve higher perceptual levels of sensory processing and cognition. We take the model versions to represent bridges between the postural data and the psychophysical thresholds data, which justify the assumption of an action-perception congruency.

The corresponding experiments with vestibular loss patients suggest to us that plantar pressure cues can largely substitute the vestibular cues while standing on stationary support. On a BSR platform where proprioceptive feedback is disabled and the platform is moving, in contrast, patients show clearly abnormal responses with extremely high gain. Model simulations helped us to relate the latter responses to an abnormal tendency for resonance of the control loop.

The results show that complex sensorimotor mechanisms such as postural control can be better understood when the experiment is formalised into a dynamic model and simulated. This applies especially when non-linearities such as thresholds are involved. With simulation the problem of a mathematical treatment of the non-linearities does not arise (see [Introduction](#)).

Acknowledgments The authors wish to thank all of the subjects who gave their time to these experiments. Supported by DFG Me 715/5-1,2. Part of this work was performed within the scope of the thesis of A. Blümle (Blümle 2004).

Appendix

The postural control model used for simulation of the present experiments is shown in Fig. 5. It represents a version of the model we used earlier to describe the responses of normal subjects and vestibular loss patients to pull and tilt stimuli (Mergner et al. 2003). In this study we assessed whether it is able to describe, in addition, the responses to visual stimuli and explain the saturation behaviour of the visual responses by thresholds in the processing of the vestibular and somatosensory signal (the proprioceptive signal was originally without threshold).

The model in Fig. 5 considers exclusively motion in the sagittal plane. It comprises a PHYSICS part and a SUBJECT part. The PHYSICS part (see also inset) includes two mutually coupled pendulums, one being the body segment ('inverted pendulum'), which consists of head, trunk and legs and is located above the other pendulum which is the foot-platform segment (primary orientations, upright and level, respectively). Both segments are interconnected by a joint (ankle joint), and only rotations around this joint are considered. As long as the body shows only small angular excursions about the upright position, gravity presses the foot firmly on the support.

With the platform level and held stationary in space, i.e. the *stationary platform* condition in our experiment (foot-in-space angle, $FS=0^\circ$), the body-to-foot angle (BF; i.e. the reverse of the foot-to-body angle, FB; $FB = -BF$) is coupled 1:1 to the body-in-space angle (BS). However, if FS is made to exactly match BS, the coupling is eliminated and the foot-to-body angle becomes "frozen" ($FB = -BF = 0^\circ$; this is mimicked in the figure simply by making $FS=0^\circ$ and opening the switch

BSRP, which corresponds to the BSR platform condition).

The angle FB is transformed by the box BIOM (for biomechanics) into a torque at the ankle joint *via* elastic and viscous elements of the muscles and ligaments of this joint (assumed to be low, see below). This torque combines with the active MUSCLE TORQUE at the joint (the summing junction of the two torques represents here the ankle joint, assuming an ideal actuator; the minus sign of the MUSCLE TORQUE signal represents the negative effect of the sensory feedback loop to be described below). The ankle joint torque acts on the box BODY INERTIA where it is transformed into the angular displacement BS ($T/J = d^2BS/dt^2$; T , torque; J , body inertia, calculated from our subjects mean values for COM and COM height above the joint; BS resulting from double integration). BS increases the torque via the box GRAVITY by the gravitational acceleration of the COM ($mgh \sin(BS)$; m , COM mass; h , COM height). The torque also leads to an a-p shift of the centre of pressure (box COP).

The perturbing stimulus applied to the system stems from an angular displacement of a visual scene in space (VS). The effect of VS on the body (visual scene with respect to body, VB) depends on BS, $VB = VS - BS$. The visual stimulus VB and its physiological effects were not contained in our original model (Mergner et al. 2003) and has been added here. On the other hand, the original model contained a contact force (pull) stimulus, which was not used in the present experiments and therefore is omitted here.

The afferent interface between the PHYSICS part and the SUBJECT part of the model is given by the four sensors. We assume that BF is sensed by ankle proprioception (*PROP*), BS by the vestibular system (*VEST*), the shift of COP by plantar somatosensory receptors (*SOMAT*) and the visual stimulus VB by the visual system (*VIS*). The hypotheses for the first three sensors were presented before (Mergner et al. 2003; Mergner 2004). In short, *PROP* is taken to stem mainly from spindle receptors in the ankle joint muscles and to inform the brain about the angle BF (internal representation, bf) with broad band-pass frequency characteristics (1 in box *PROP*, ideal transfer characteristics; sign reversal, -1 , changes $FB = -BF$ into BF). *VEST* is thought to provide an internal estimate of BS, i.e. signal bs, which for the present purpose is taken to show broad band-pass characteristics (box *VEST* with ideal transfer characteristics, 1). *SOMAT* is represented by plantar somatosensory receptors which provide a low-pass filtered estimate of COP shift at the foot soles (note low-pass filter symbol in box *SOMAT*; further details in Maurer et al. 2000, 2001; Mergner 2004; in the box the COP signal is multiplied with the factor $-[mg]$). The newly implemented sensor *VIS* is thought to yield an internal estimate of body motion with respect to the visual scene (bv), which is sign reversed with respect to VB (-1 in box *VIS*) and shows

low-pass filter characteristics (see Introduction and legend of Fig. 7).

The efferent interface between the two parts of the model is given by the box PDI, which represents a “neural controller” with proportional, differential and integrative properties (values of factors K_P , K_D and K_I , respectively, are given in the legend of Fig. 5; the above mentioned elastic and viscous elements in box BIOM were taken to be 10% of K_P and K_D , respectively, as suggested in the study of Peterka 2002). The box PDI transforms a neural command signal into torque at the ankle joint. The neural command signal carries a single delay time (box Δt ; 100 ms). This reflects our assumption that the brain has found ways to deal in a simplified way with the many different time delays in the system.

The SUBJECT part of the model contains a summing junction at which five signals are combined. The first would be the proprioceptive *bf* signal which we consider to form, together with the system’s efference, a ‘local feedback loop’ that stabilises the joint and, with the values used for K_P and K_D , takes into account body inertia. The other signals represent internal estimates of the external stimuli. One stimulus would be the gravity effect on the body, which internally is represented by the vestibular *bs* signal. It carries a gain factor (G_2) and position threshold (T_2). Another external stimulus would be FS when it is made to follow BS in the BSR platform condition (with stationary platform, in contrast, it need not be represented here internally, since then $FS = 0^\circ$). The internal representation of FS is internally derived from a vestibular-proprioceptive signal fusion in the form of $fs = bs - bf$ (*fs* signal). The fusion is thought to originate from vestibular and proprioceptive velocity signals and fs therefore carries a velocity threshold (T_1 ; furthermore the gain factor G_1). The signals bs and fs are thought to be missing in vestibular loss patients (inactivation of dark grey box in the model of Fig. 5).

The *bv* signal, i.e. the sign-reversed estimate of the visual stimulus VB (third external stimulus), is thought to carry a velocity saturation, in analogy to what is known about the optokinetic reflex (see Introduction). As mentioned in the Discussion, we assume that the visual signal interacts with the vestibular signal, yielding a ‘sensory weighting’ of the two signals. At the present stage of our work, however, we refrained from implementing such a mechanism here and adjusted, instead, the gain of the *bv* signal (G_4) to fit the simulated data to the experimental data for each experimental condition.

The *bs*’ signal is derived from the *SOMAT* sensor. In the original model, this signal was used for two functions (see Mergner et al. 2003). One function applied to the stationary platform condition and consisted of interactions with the vestibular signal (not shown here). By way of these interactions, gravity is counteracted by a fused vestibular and somatosensory signal (here represented by the vestibular bs signal alone, for simplification) and, furthermore, an internal estimate of those body excursions is created, which are produced by external contact

forces such as a pull stimulus (not applicable here). In the situation with BSR platform, these functions become replaced by another function which consists of a balancing in direct relation to the COP shifts (recall that ankle torque rather than ankle angle adjustments are to be used for balancing in this platform condition; the presumed change in 'postural strategy' helped us to describe in the previous study pronounced phase shifts of the centre of pressure, COP, at low stimulus frequencies). Thus, in the present model normals use the SOMAT signal only in the BSR platform condition. In the model of Fig. 5, the switching from a vestibular (bs) graviceptive compensation on stationary platform to a somatosensory one (*bs'*) on the BSR platform was achieved by setting the thresholds T2 from 0.06° to ∞° and, vice versa, the thresholds T3 from ∞° to 0.06° .

We have redrawn the model of Fig. 5 in the four panels of Fig. 7 (a–d) for the four experimental conditions used (platform stationary or BSR; vestibular system present or absent), removing those parts which are inactive in a given condition. Furthermore, for simplification we omitted the biomechanical part and fused the boxes BODY INERTIA and GRAVITY to one box. *Panel a* shows the model of normal subjects on the stationary platform. The signal fs, i.e. the internal representation of FS, is omitted since $FS = 0^\circ$. Furthermore, the SOMAT sensor signal is not used (SOMAT box crossed out; compare above, *bs'* signal). *Panel b* shows the model of normal subjects on the BSR platform. As described before, proprioceptive feedback is disabled in this condition (crossed box PROP). By this, subjects can use only the vestibular feedback for the fs signal in order to cope with the platform motion. Furthermore, the gravitational body acceleration is counteracted with the help of the *bs'* signal from the SOMAT sensor, rather than with the vestibular bs signal (which therefore is omitted).

Panel c shows the model of patients on the stationary platform. Since patients have no vestibular bs signal to counteract the gravitational body acceleration (VEST sensor crossed) they use the *bs'* signal from the SOMAT sensor instead (in terms of an adaptation). *Panel d* shows the model of patients on the BSR platform. The situation is as in panel c, but proprioceptive feedback is disabled (PROP sensor crossed) and patients have no fs signal to cope with the platform motion.

As described in the Discussion, we performed simulations of our model for the four experimental conditions and adjusted in it the gain of the visual signal (G4) in order to fit the simulated data to the experimental data and successfully achieved this for all four conditions. In particular, the saturation characteristics of the visual responses were also well mimicked and the simulations helped us to understand better how these characteristics are brought about (see Discussion). Furthermore, we found the gain of the visual signal to be low, a finding which suggests that subjects suppressed the signal to a large extent (exception: patients on BSR platform, where they obviously used the visual scene as a

space reference for their posture control although it was moving).

In addition, we applied an automatised parameter identification procedure to the visual path in the model. The procedure varied the values of the corner frequency of the first order low-pass filter, of the velocity saturation and of the gain in the path, using the Matlab Optimization toolbox function 'fminsearch' (which is based on the so-called simplex search method of Nelder-Mead; see Lagarias et al. 1998). Using the filter, saturation and gain values given in the Discussion as initial estimates, the procedure searched the minimum deviation of the simulated visual responses from the corresponding experimental data (in polar coordinates). Each iteration of the procedure was applied to the 20 responses (one response for each of the five stimulus amplitudes and the four frequencies) and a scalar error function was evaluated. Then, the procedure changed the filter, saturation and gain values and the error function was re-evaluated. This sequence was repeated until the error functions of the three parameters were minimized.

Changing, during the procedure, the corner frequency of the low-pass filter yielded no considerable effect on the fits. In contrast, changing the velocity saturation yielded clear effects; lowering of the initial estimate of $3^\circ/s$ to approximately $1^\circ/s$ improved the fit slightly, and this occurred similarly in the four experimental conditions. Also changing the visual gain values improved the fit with the final estimates being clearly different across the experimental conditions (values were given in Discussion).

When repeating the procedure separately for the five different stimulus amplitudes used, we noted that the value of the calculated gain estimate showed no consistent dependency on stimulus amplitude. In contrast, the error remaining after the fit decreased with increasing stimulus amplitude (it amounted to 0.56, 0.24, 0.13, 0.07 and 0.04 for the $\pm 0.25^\circ$, $\pm 0.5^\circ$, $\pm 1^\circ$, $\pm 2^\circ$ and $\pm 4^\circ$ stimuli, respectively). The error was defined here as the mean distance between the experimental and the simulated data points (Fourier transformed, in polar coordinates, across all amplitudes and frequencies) after normalisation to the corresponding stimulus. The error in absolute values, however, was similar across the five stimuli. This suggests that it was mainly determined by spontaneous sway.

References

- Akiduki H, Nishiike S, Watanabe H, Matsuoka K, Kubo T, Takeda N (2003) Visual-vestibular conflict induced by virtual reality in humans. *Neurosci Lett* 340:197–200
- Amblard B, Cremieux J, Marchand AR, Carblanc A (1985) Lateral orientation and stabilization of human stance: static versus dynamic visual cues. *Exp Brain Res* 61:21–37
- van Asten WNJC, Gielen CCAM, Denier van der Gon JJ (1988) Postural adjustments induced by simulated motion of differently structured environments. *Exp Brain Res* 73:371–383

- Barnes GR (1993) Visual-vestibular interaction in the control of head and eye movement: the role of visual feedback and predictive mechanisms. *Prog Neurobiol* 41:435–472
- Benson AJ, Hutt ECB, Brown SF (1989) Thresholds for the perception of whole body angular movement about a vertical axis. *Aviat Space Environ Med* 60:205–213
- Bles W, Kapteyn TS, Brandt T, Arnold F (1980) The mechanism of physiological height vertigo. II. Posturography. *Acta Otolaryngol* 89:534–540
- Bles W, Vianney de Jong JM, de Wit G (1983) Compensation for labyrinthine defects examined by use of a tilting room. *Acta Otolaryngol* 95:576–579
- Blümle A (2004) Interaktion der visuellen, somatosensorischen und vestibulären Sinnessysteme bei der Gleichgewichtsregulation. Doktorarbeit, University of Freiburg, URL: <http://freidok.uni-freiburg.de/volltexte/1219/>, URN: urn:nbn:de:bsz:25-opus-12199
- Dichgans J, Brandt T (1979) Visual-vestibular interaction: effects on self-motion perception and postural control. In: Held R, Leibowitz H, Teuber HL (eds) *Handbook of sensory physiology*, vol VIII. Springer, Berlin Heidelberg New York, pp 755–804
- Fitzpatrick R, McCloskey DI (1994) Proprioceptive, visual and vestibular thresholds for the perception of sway during standing in humans. *J Physiol* 478:173–186
- Keshner EA, Kenyon RV (2000) The influence of an immersive virtual environment on the segmental organization of postural stabilizing responses. *J Vestib Res* 10:207–219
- van der Kooij H, Jacobs R, Koopman B, van der Helm F (2001) An adaptive model of sensory integration in a dynamic environment applied to human stance control. *Biol Cybern* 84:103–115
- Kotaka S, Croll GA, Bles W (1986) Somatosensory ataxia. In: Bles W, Brandt T (eds) *Disorders of posture and gait*. Elsevier, New York, pp 178–183
- Kuno S, Kawakita T, Kawakami O, Miyake Y, Watanabe S (1999) Postural adjustment response to depth direction moving patterns produced by virtual reality graphics. *Jpn J Physiol* 49:417–424
- Lagarias JC, Reeds JA, Wright MH, Wright PE (1998) Convergence properties of the Nelder-Mead Simplex Method in low dimensions. *SIAM J Optim* 9:112–147
- Lee DN, Lishman JR (1975) Visual proprioceptive control of stance. *J Hum Mov Stud* 1:87–95
- Lestienne F, Soechting J, Berthoz A (1977) Postural readjustments induced by linear motion of visual scenes. *Exp Brain Res* 28:363–384
- Lord SR, Menz HB (2000) Visual contributions to postural stability in older adults. *Gerontology* 46:306–310
- Maurer C, Mergner T, Bolha B, Hlavacka F (2000) Vestibular, visual, and somatosensory contributions to human control of upright stance. *Neurosci Lett* 281:99–102
- Maurer C, Mergner T, Bolha B, Hlavacka F (2001) Human balance control during cutaneous stimulation of the plantar soles. *Neurosci Lett* 302:45–48
- Maurer C, Mergner T, Peterka RJ (2004) Abnormal resonance behaviour of the postural control loop in Parkinson's disease. *Exp Brain Res* 157:369–376
- Mergner T (2004) Meta level concept versus classic reflex concept for the control of posture and movement. *Arch Ital Biol* 142:175–198
- Mergner T, Siebold C, Schweigart G, Becker W (1991) Human perception of horizontal head and trunk rotation in space during vestibular and neck stimulation. *Exp Brain Res* 85:389–404
- Mergner T, Bergmann T, Rumberger A, Maurer C, Otte M, Hünemörder U (1997) Anwendung von Virtual Reality und Stereo-Video in Echtzeit bei der Untersuchung der Gleichgewichtsregulation des Menschen. In: Saupe D (ed.) *Proceedings 5th workshop for digital image processing in medical sciences (Digitale Bildverarbeitung in der Medizin)*. Zentralstelle für Forschungsförderung und Technologietransfer, Albert-Ludwigs-Universität Freiburg, pp 57–62. ISBN 3-9805054-2-1
- Mergner T, Schweigart G, Müller M, Hlavacka F, Becker W (2000a) Visual contributions to human self-motion perception during horizontal body rotation. *Arch Ital Biol* 138:139–166
- Mergner T, Wertheim A, Rumberger A (2000b) Which retinal and extra-retinal information is crucial for circularvection? *Arch Ital Biol* 138:123–138
- Mergner T, Nasios G, Maurer C, Becker W (2001) Visual object localisation in space: interaction of retinal, eye position, vestibular, and neck proprioceptive information. *Exp Brain Res* 141:33–51
- Mergner T, Maurer C, Peterka RJ (2003) A multisensory posture control model of human upright stance. *Prog Brain Res* 142:189–201
- Nashner LM (1972) Vestibular postural control model. *Kybernetik* 10:106–110
- Norre ME (1993) Sensory interaction testing in platform posturography. *J Laryngol Otol* 107:496–501
- Paulus WM, Straube A, Brandt T (1984) Visual stabilization of posture. Physiological stimulus characteristics and clinical aspects. *Brain* 107:1143–1163
- Peterka RJ (2000) Postural control model interpretation of stabilogram diffusion analysis. *Biol Cybern* 82:335–343
- Peterka RJ (2002) Sensorimotor integration in human postural control. *J Neurophysiol* 88:1097–1118
- Peterka RJ, Benolken MS (1995) Role of somatosensory and vestibular cues in attenuating visually induced human postural sway. *Exp Brain Res* 105:101–110
- Peterka RJ, Loughlin PJ (2004) Dynamic regulation of sensorimotor integration in postural control. *J Neurophysiol* 91:410–423
- Schweigart G, Mergner T, Barnes G (1999) Eye movements during combined pursuit, optokinetic and vestibular stimulation in macaque monkey. *Exp Brain Res* 127:54–66
- Schweigart G, Mergner T, Barnes GR (2003) Object motion perception is shaped by the motor control mechanism of ocular pursuit. *Exp Brain Res* 148:350–365
- Tossavainen T, Juhola M, Pyykko I, Aalto H, Toppila E (2003) Development of virtual reality stimuli for force platform posturography. *Int J Med Inf* 70:277–283
- Winter DA (1990) *Biomechanics and motor control of human movements*, 2nd edn. Wiley, New York